FAKULTA TEXTILNÍ TUL

MULTIFUNCTIONAL CARBON BASED FELT

Yuanfeng Wang, M.Eng.

SUMMARY OF THE THESIS

Title of the Ph.D. thesis:	Multifunctional Carbon Based Felt
Author:	Yuanfeng Wang, M.Eng.
Field of Study:	Textile Technics and Material Engineering
Mode of Study:	Full-time
Department:	Department of Material Engineering
Supervisor:	prof. Ing. Jiří Militký, CSc.

Committee for defense of the dissertation:

předseda:	
prof. Ing. Michal Vik, Ph.D.	FT TUL Department of Material Engineering
místopředseda:	
prof. Dr. Ing. Zdeněk Kůs	FT TUL, Department of Clothing Technologies
doc. Ing. Maroš Tunák, Ph.D.	FT TUL, Department of Textile Evaluation
doc. RNDr. Jiří Vaníček, CSc. (opponent)	
assoc. prof. Guocheng Zhu, Ph.D.	Zheijang Sci Tech University, School of Materials Science and Engineering, Hangzhou, China
Ing. Karel Kupka, Ph.D.	TriloByte Statistical Software, s.r.o.
Ing. Josef Večerník, CSc.	Večerník s.r.o.

The second opponent who is not a member of the committee

prof. Lin Liu, Ph.D.	Zheijang Sci Tech University, School of Materials Science and Engineering, Hangzhou, China

The dissertation is available at the Dean's Office FT TUL.

Liberec 2024

Abstract

Pyrolysis has emerged as a strategy for processing waste textiles, with the conversion of high-carbon-content textile waste into carbonaceous materials being beneficial for recovering its economic value while mitigating the environmental impact of textile waste. Carbon felt is widely used due to its lightweight nature and internal 3D conductive network. However, limited research exists on directly using waste textile felts as a precursor to produce carbon felt. The aim of this thesis is to carbonize acrylic-based waste felts under controlled conditions to produce carbon felt and enable its multifunctional applications. To achieve the conversion of acrylic-based felts into flexible carbon felts with excellent performance, this study aims to investigate the impact of different loading tension methods and PTFE coatings during the pyrolysis process on the shrinkage rate, mechanical properties, electrical properties, and thermal properties of the resulting carbon felt. The results indicate that applying edge load to the samples during the carbonization stage helps to reduce the shrinkage rate of the final product, allowing the carbon felt to gain flexibility and form a well-structured conductive network.

To study the impact of PTFE coating on the pyrolysis of acrylic -based felts, acrylic -based felts were coated with different concentrations of PTFE and subsequently subjected to pyrolysis. By examining the morphology, mechanical properties, and electrical properties of PTFE-coated samples, we found that higher coating concentrations had a greater impact on the performance of the resulting carbon felt. Although high coating concentrations increased the material's modulus and electrical conductivity, they also led to a loss of flexibility in the carbon felt, which could severely limit its application scope. By characterizing the morphology and structure of carbon felts prepared at different carbonization temperatures under an edge loading mode, it was found that increasing the carbonization temperature promoted higher crystallinity within the fibers and the formation of an ordered graphite structure. The formation of a dense, highly conductive network and high porosity was achieved. EMI shielding results demonstrated that the resulting carbon felt achieved a high EMI shielding effectiveness of 55 dB and a specific shielding effectiveness of 2676.9 dBcm^{2}g^{-}1, surpassing many carbon composites. Additionally, the carbon felt exhibited excellent heating efficiency and high heating rates in resistive heating tests. Structural stability was investigated through a custom-designed experiment. The results showed that even under heating conditions, the carbon felt could maintain internal conductive pathway stability through multiple bending cycles.

This work also investigated the feasibility of converting acrylic -based filter felts into carbon felts for use in respiratory filtration layers. The excellent electrical conductivity of carbon felt allows it to be used not only as a respiratory filtration layer but also for high-temperature

electrical disinfection. The design of the mask body and the corresponding electrode configuration enabled controlled resistive heating performance, ensuring the reliability of high-temperature disinfection of the carbon felt. Filtration efficiency and antibacterial testing results showed that the carbon felt achieved over 90% filtration efficiency for inhalable particles and effectively inhibited microbial growth due to its antibacterial properties. Flexible carbon felt offers lower manufacturing costs and exhibits good chemical and structural stability. Functional testing results indicate that it demonstrates significant potential for applications in wearable heaters, flexible EMI shielding, respiratory filters, and other related fields.

Keywords:
acrylic based waste felts, PTFE coating, special pyrolysis, electrical conductivity, EMI shielding, ohmic heating, respiratory filters

Anotace

Pyrolýza se běžně používá jako strategie pro zpracování odpadních textilií, přičemž přeměna textilního odpadu s vysokým obsahem uhlíku na uhlíkaté materiály je potřebná pro přípravu ekonomicky výhodných produktů s vyšší užitnou hodnotou („upcycling“) a zároveň zmírňuje dopad textilních odpadů na životní prostředí. Uhlíkové plsti jsou široce používána pro svoji relativně nízkou hmotnost a vysokou elektrickou vodivosti díky vnitřní 3 D vodivé síti. Přímé použití odpadních textilních plstí jako prekurzoru k výrobě uhlíkových plsti je však zkoumáno jen omezeně. Cílem této dizertační práce je optimalizace karbonizace odpadních plstí na bázi acrylic za kontrolovaných podmínek pro výrobu uhlíkových plstí a realizaci jejích multifunkčních aplikací. Byl zkoumán vliv různých metod zatížení odpadních plstí na bázi akrylových vláken s PTFE zátěrem na proces smršťování při pyrolýze. Byly hodnoceny mechanické vlastnosti, elektrické vlastnosti a tepelné vlastnosti finální uhlíkové plsti. Výsledky naznačují, že aplikace okrajového zatížení na vzorky během fáze karbonizace pomáhá snížit rychlost smrštění konečného produktu, což umožňuje uhlíkové plsti získat pružnost a vytvořit dobře strukturovanou vodivou síť. Pro studium vlivu zátěru PTFE na pyrolýzu plstí na bázi akrylových vláken byly plsti potaženy různými koncentracemi PTFE a následně podrobeny pyrolýze. Zkoumáním morfologie, mechanických vlastností a elektrických vlastností vzorků potažených PTFE bylo zjištěno, že vyšší koncentrace povlaku měly pozitivní dopad na mechanické a elektrické vlastnosti výsledné uhlíkové plsti. Vysoké koncentrace povlaku však vedly také ke ztrátě pružnosti uhlíkové plsti, což by mohlo vážně omezit jejich použitelnost. Zkoumáním morfologie a chování uhlíkových plstí připravených při různých teplotách karbonizace v režimu zatížení okraje bylo zjištěno, že zvýšení teploty karbonizace podpořilo růst krystalinity ve vláknech a tvorbu uspořádané grafitické struktury. Bylo dosaženo vytvoření husté, vysoce vodivé sítě s vysokou porozitou. Výsledky stínění elektromagnetického záření (EMI) prokázaly, že výsledná uhlíková plsť dosáhla vysoké účinnosti stínění EMI 55 dB a specifické účinnosti stínění 2676,9 $dBcm^2g^{-}1$, čímž překonala mnoho uhlíkových kompozit. Kromě toho uhlíková plsť vykazovala vynikající účinnost ohmického ohřevu a vysoké rychlosti ohřevu. Strukturální stabilita byla zkoumána pomocí speciálně navrženého experimentu. Výsledky ukázaly, že si uhlíková plsť udržela stabilitu vnitřních vodivých drah po více cyklech ohybu. Bylo také zkoumáno využití připravených uhlíkových plstí pro tvorbu filtračních vrstev použitelných v respirátorech a filtračních maskách (filtrace vzduchu). Vynikající elektrická vodivost uhlíkové plsti umožnila její použití nejen jako respirační filtrační vrstvu, ale také pro vysokoteplotní elektrickou dezinfekci kontaminantů a mikrobů/virů. Konstrukce masky a vhodná konfigurace elektrod umožnila řízený odporový ohřev, zajišťující spolehlivost vysokoteplotní dezinfekce uhlíkové plsti. Účinnost filtrace a výsledky antibakteriálních testů ukázaly, že uhlíková plsť dosáhla více než 90 % účinnosti filtrace pro inhalovatelné částice a

účinně inhibovala výskyt mikrobů. Flexibilní uhlíkové plsti mají obecně nižší výrobní náklady a vykazují dobrou chemickou a strukturální stabilitu. Výsledky funkčních testů ukázaly, že připravené uhlíkové plsti mají významný potenciál pro aplikace v oděvních ohřívačích, flexibilním stínění EMI, respiračních filtrech a dalších typech funkčních materálů.

Klíčová slova:
odpadní plsti na bázi akrylu, zátěr PTFE, speciální pyrolýza, elektrická vodivost, EMI stínění, ohmický ohřev, respirační filtry.

Summary

1 Introduction

The flourishing of smart textile materials has spurred the development of flexible and lightweight conductive fiber materials. Carbon materials are undoubtedly the preferred choice for meeting the aforementioned performance requirements. Carbon fibers can be prepared by carbonizing or graphitizing polymers with high carbon content [1]. Approximately 90% of carbon fiber production comes from acrylic precursors, though cellulose and pitch are also used as precursors for carbon fiber [2]. This is because acrylic exhibits high carbonization yield, excellent fiber-forming properties, and unique thermal chemical characteristics, allowing for the synthesis of large graphite planes during pyrolysis. acrylic-based carbon fiber production involves thermal oxidation stabilization of the fibers in air conditions within the temperature range of 200-400 °C, followed by carbonization of the fibers at high temperatures between 800 °C and 1700 °C [3].

Carbon fibers are primarily used in two forms. One uses bundles of carbon fibrous filaments to create carbon fabric composites, typically with a resin matrix. In this application, carbon fibers mainly provide their exceptional mechanical properties to the composite material. Another form is carbon felt, in which fibers are combined through processes such as condensing, pressing, and needle punching. In addition to the inherent properties of carbon fibers, carbon felt also possesses a stable three-dimensional network structure, excellent flexibility and high porosity, which has led to its widespread application [4][5].

The manufacturing process of carbon felt include the formation of felt via needle punching and high-temperature carbonization. Most carbon felt manufacturing directly uses pre-carbonized fibers as raw materials, requiring only the felting process to produce carbon felt [6][7]. There has also been a study reporting the use of pre-oxidized acrylic fibers to produce felt, followed by carbonization [8]. acrylic felt is widely used in fiber filtration materials. Using waste acrylic felt as a precursor for carbon felt not only saves on raw material costs but also eliminates the need for fiber opening, carding, and felting processes. More importantly, this strategy transforms waste fibers into high-value materials, effectively alleviating the environmental impact of solid fiber waste. However, there are relatively few reports on the preparation of carbon felt through the carbonization of acrylic felt. This is because fibers tend to shrink during pyrolysis, and using already-formed fiber assemblies as carbonization raw materials often leads to the production of hard or brittle carbon materials. Therefore, controlling the pyrolysis of waste acrylic felt through certain measures during experimental processes to produce flexible and conductive carbon felt holds significant research value.

As an industrial textile, acrylic felt typically undergoes functional finishing treatments, which leads to complex material composition. This complexity poses challenges when using it as a precursor for carbon fiber production, but it also opens up new avenues for exploration. Some

studies have shown that using mixed fibers as precursors for carbon felt optimizes its mechanical properties[9]. Compared to pure acrylic felt precursors, acrylic felt with polymer coatings may exhibit different properties after carbonization, yet research in this area is lacking.

Furthermore, as a fiber material with excellent electrical conductivity, carbon felt possesses significant advantages in terms of lightweight and flexibility over metals. Its potential applications in resistive heating, electromagnetic shielding, filtration, and other areas are also worthy of research consideration.

2 Purpose and the aim of the thesis

This work aims to investigate the parameters involved in the preparation process of carbon felt from acrylic felt and explore the multifunctionality of carbon felt. The specific objectives of this study are as follows:

2.1 Pyrolysis of acrylic-based felt coated by layer of PTFE

Investigation of different loading modes to acrylic-based felt during the carbonization stage and their impact on the shrinkage rate, mechanical properties, electrical conductivity, and thermal conductivity of the resulting samples. Preparation of carbon felt derived from acrylic-based felt with PTFE coatings and evaluation the impact of the coatings on shrinkage and mechanical properties.

2.2 Flexible carbon felt characterization and properties

Comprehensive study of the EMI shielding efficiency, mechanical properties and resistive heating behavior of the resulting carbon felts. Testing of the structural stability of the samples after multiple bending cycles through a custom-designed experiment.

2.3 Special application of the prepared carbon felt

Design of carbon felt as a filtration layer for respirator filtration system. Examination of the breathability and vapor permeability of the carbon felt. Disinfection of the carbon felt via resistive heating after filtration.

3 Overview of the current state of the problem

Carbon materials are a class of materials composed of carbon elements that exhibit exceptional performance due to their unique hybridization orbitals and diverse structures. Carbon possesses four valence electrons, which can form strong covalent bonds with other elements through hybridization orbitals. Carbon's hybridization orbitals include sp^3, sp^2, and sp hybridization, corresponding to carbon structures such as diamond, graphite, and acetylene, respectively. The different hybridization orbitals lead to the rich and varied physical and chemical properties of carbon materials. This has rendered carbon materials highly versatile for a broad spectrum of applications and has garnered significant research attention.

The production of carbon materials is typically achieved through the high-temperature pyrolysis of precursors. Recently, there has been an increased focus on developing new pathways for carbon materials that are more environmentally friendly. Polymer molecules in textile fibers typically contain a high carbon content, which can yield solid carbon products through pyrolysis under certain conditions. The strategy of producing carbon materials from textile waste not only reduces the production cost of carbon materials but also serves as a method of managing textile waste, thereby contributing to the valorization of textile waste. A considerable amount of research has been conducted on the preparation of carbon materials using textile waste as a carbon source, including cotton [10], polyester [11], acrylic [12][13], flax [14], and blended fabrics [15].

Acrylic (or polyacrylonitrile) precursor is the primary material used in the preparation of conductive carbonized fiber materials. The production of carbon fibers using acrylic-based fibers typically involves three processes: stabilization, carbonization, and graphitization. It is well known that applying appropriate tension to acrylic fibers during the during the carbon fiber production process facilitates the preferred orientation of the fibers, thereby enhancing the strength and tensile modulus of the resulting carbon fibers. The influence of tension, especially during the stabilization process, on carbon fibers has been extensively studied [16][17][18]. Furthermore, the tensile stress also alleviates the contraction of the fibers due to high temperatures [19].

In traditional carbon fiber production using acrylic precursor filaments, the application of tension only requires control of the two ends of the filament during the high-temperature treatment process. The method of applying tension is not feasible for the already-formed acrylic precursor felt. This is because the fiber arrangement within the felt is non-directional and there is significant entanglement between fibers. The thermal degradation process of the fiber material inevitably leads to shrinkage and even breakage. Therefore, preserving the fiber morphology of the original felt to some extent during production to ensure the mechanical properties of the resulting carbon felt is a challenge. In this area, current research is relatively limited. Baheti et al. found that applying pre-tension on the felt during the stabilization process mitigates the shrinkage rate of the

resulting carbon web [20]. However, this study did not provide a specific method for applying pre-tension, and the resulting samples were relatively brittle and fragile. Other studies have also presented various methods of applying tension to acrylic nanofiber webs during the stabilization process, including vertical loaded hanging [21], both-sides hanging [22], borders fixation [23], and sandwiching between graphite plates [24]. Applying vertical tensile force during the stabilization phase has been found to help control the shrinkage rate of the fibers and aid in the orientation of macromolecular chains within the fibers, thereby leading to the development of high tensile modulus fibers. The authors believed that the technique of applying tensile force to electrospun acrylic fibers during the stabilization process was effective in producing relatively large-sized stabilized fiber mats compared to other techniques [21]. Ehrmann et al. studied the impact of edge fixation on samples during the stabilization process. They found that the change in the area of the fixed samples was smaller as the stabilization temperature and heating rate increased[23].

The use of a metal substrate to provide single-sided or double-sided support during the stabilization process for electrospun acrylic fiber mats has been proposed by Storck et al. [25]. The results indicate that stabilization and carbonization within a double-sided metal-supported sandwich structure preserve the original fiber morphology and even accelerate the carbonization process. However, the carbonization temperature in this work was only 500 °C, significantly lower than the typical preparation temperature for carbon felt. The same research team further increased the carbonization temperature and utilized different metal and metalloid substrates for the sandwich structure [26]. However, their study was primarily focused on finding the optimal balance between carbonization, crystallinity, and intact nanofibers, and did not investigate the mechanical properties such as the flexibility of the resulting samples. It can be stated that current research primarily focuses on applying tension during the stabilization process of fiber mats, while there is a lack of reporting on tension application during the carbonization stage. Furthermore, no studies have been found regarding the mechanical properties such as tensile strength and flexibility of the carbon felt or carbon nanofiber network obtained after applying tension. Applying tension to samples during the carbonization phase has research value as a potential means of enhancing the mechanical properties of carbon felt. Identifying an appropriate method could enable the direct preparation of carbon felt from textile waste felt precursors without brittle limitations, thereby avoiding additional processing steps such as opening and mixing.

In addition, the aforementioned studies have all utilized electrospun nanofibers as precursors without taking into consideration the cost-effectiveness of the precursor material in the carbon felt fabrication process. Choosing discarded textiles as precursors for carbon material not only reduces manufacturing costs but also contributes to environmental sustainability through textile recycling, thereby minimizing environmental impacts. Acrylic fiber is not only used in textile for clothing,

but it can be found in industrial textiles where it is often manufactured into felt for use as filtration material or dust collectors. Utilizing discarded industrial acrylic felts as precursors for carbon felts represents a novel approach to achieving their high-value reutilization. As an industrial textile, acrylic felt typically undergoes functional finishing treatments to enhance mechanical properties and improve waterproof and oil-resistant effects. This results in a complex composition of the material. Such a complexity poses challenges when used as a precursor for carbon fiber production but also opens up new avenues for exploration. A recent study reported that when using blend of acrylic and Kevlar fibers as the precursor for carbon felt preparation, lower stiffness, shrinkage and dusting behavior were found on the resulting product[9]. This presents us with an academic insight: Employing pure acrylic as the precursor material often leads to carbon materials with inherent stiffness and brittleness. However, through the amalgamation with other high-performance materials, acrylic serves to ensure an exceptional carbon yield, thereby imparting electrical conductivity to carbon felts. The application of high-performance finishing agents subsequently enables the optimization of mechanical properties.

4 Used methods, study material

4.1 Materials

The needle-punched acrylic-based dust filter felt used as the precursor in this work was purchased from Zhejiang Hengze Filter Material Co., Ltd, China. The density of the felt is 500g/m^2 and the thickness is 2.0- 2.1 mm, where the acrylic-based fibers have a diameter of 12-16 μm. One side of the felt is coated with polytetrafluoroethylene (PTFE) at a thickness of about 0.1 mm. The other chemicals used are of reagent grade.

4.2 Sample preparation

4.2.1 Carbon felt prepared by different loading mode

The precursor material for carbon felt, acrylic-based felt, was washed and cut into squares pieces before the experiment. First, the acrylic-based felt was stabilized in an air atmosphere using a muffle furnace at a temperature of 200°C for 2 hours. During the stabilization process, the sample was placed between two metal plates to maintain its original flat shape. Subsequently, the carbonization of the stabilized acrylic-based felts was carried out in a muffle furnace under nitrogen atmosphere at a temperature of 800-1100 ℃ for 30-90 min with a heating rate of 10 °C/min. The samples were labeled as AC_x, where x represented the carbonization temperature. Here, during the carbonization process, two modes were used to apply tension to the fibers in the felt. One is simply placing cylindrical blocks weighing 66g at each of the four corners of the sample, termed as the edge loading. Another mode is to use a flat crucible with weight of 540g as a load to completely cover the sample surface, termed as uniform loading. Samples without any loading were also prepared as control samples.

4.2.2 Carbon felt prepared from acrylic-base felt with PTFE coating.

To study the impact of the PTFE coating on carbonization, the acrylic-based felt was first subjected to a coating process. Dip-pad-dry method was used for the PTFE coating of acrylic-base felt. Briefly, a PTFE dispersion of 60wt% was diluted with deionized water to 3wt%, 6wt%, 12wt% and 30wt%, respectively. The felt was then immersed in PTFE dispersions of different concentrations. After thorough saturation, excess dispersion was removed using pressure rollers. Finally, the samples were dried and cured in an oven at 120 ℃.

The PTFE-coated acrylic felt was carbonized using an edge loading method under the same experimental conditions as described in the previous section, with a temperature of 800 °C and a duration of 30 min.

4.3 Characterizations

4.3.1 Morphology

The surface morphology of the carbon felts obtained in this study was examined via scanning

electron microscopy (SEM) using a VEGA3 TESCAN instrument operated at an acceleration voltage of 10 kV. Prior to testing, the sample surfaces were subjected to a metal sputtering treatment with a thickness of 10 nm. The surface elements of the resulting carbon felts were analyzed using an Oxford X-max 20 energy dispersive X-ray spectrometer (EDX).

4.3.2 Mechanical Properties

The tensile properties and stiffness of the samples were tested to study the mechanical properties of the obtained carbon felt.

In order to investigate the flexibility of the carbon felts, the stiffness of the samples was evaluated by means of a TH-5 instrument (Czech Republic), following the guidelines outlined in the standard ČSN 80 0858. The specimens utilized for the study were rectangular in shape, with a length and width of 5 and 2.5 cm, respectively. During the testing process, one end of the specimen was bent to 60°, and the bending force was measured by the instrument. The bending moment was then computed using Equation (1),

$$M_0 = F_m \times k \tag{1}$$

where M_0 [mN cm] is bending moment, F_m [mN] is bending force measured by the instrument. The constant k for a sample with a width of 2.5 cm is 0.604 cm [27].

The tensile properties of the samples were tested using the dynamometer LaborTech 2.050 (LaborTech, Czech Republic) in accordance with the EDANA 20.2-89 standard. Samples with a width of 1 cm and a clamping length of 5 cm was stretched to fracture, and the tensile force and elongation were recorded. The tensile stress [MPa] was then calculated as the ratio of the breaking force to the cross-sectional area of the sample. The calculation of modulus E [MPa] was as follows,

$$E = \lim_{\varepsilon \to 0} \frac{d\sigma}{d\varepsilon} \tag{2}$$

where σ [MPa] is the tensile stress and ε is the strain, near origin of the stress-strain curve. In the above experiment, measurements were realized five times, and the average was taken. Standard deviation was used as error bars.

4.3.3 Porosity

By measuring the bulk density and fiber density of the carbon felt and utilizing the definition of porosity, which is the ratio of the pore volume to the total volume, the porosity φ [%] of the carbon felt was calculated using Equation (3),

$$\varphi = 1 - \frac{\rho_{\text{bulk}}}{\rho_{\text{fiber}}} \tag{3}$$

where ρ_{bulk} is the bulk density[g/cm^3] of carbon felt and ρ_{fiber} is the density [g/cm^3] of fiber, respectively. The volume of the carbon fiber was determined through the immersion method, which involves immersing the fibers in water-filled containers and measuring the resulting

change in water level[28]. The thickness of the carbon felt was measured using a thickness gauge (D-2000-T, SCHMIDT). The testing head size was 20 cm², and the applied pressure was 1 kPa. The bulk volume of carbon felt was determined by multiplying the sample area by the thickness. The mass of the samples was measured using an electronic balance.

4.3.4 Air and Water Vapor Permeability

The air permeability of carbon felts was measured by FX-3300 air permeability tester (TESTEST AG, Switzerland). The testing was carried out at various pressure differences, ranging from 60 to 260 Pa, with increments of 10 Pa. Each pressure condition underwent five tests, and the average value was calculated.

The evaporation resistance R_{et} [m^2 Pa/W] were determined using the Permetest Instrument (SENSORA, Czech Republic) according to ISO 11092. A semi-permeable membrane was placed between the testing head and the sample to preserve the dryness of the sample. The heat losses were determined by measuring the change in heat flow value before and after the sample covered the testing head. The water vapor resistance R_{et} can be calculated using Equation (4)[29]

$$R_{et} = \frac{P_m - P_a}{{q_s}^{-1} - {q_0}^{-1}} \quad (4)$$

where P_m is the saturation water vapor pressure [Pa] at ambient temperature, P_a is the water vapor pressure [Pa] in the room, q_s is the heat loss [W/m^2] of the measurement head with the sample, and q_0 is the heat loss [W/m^2] of the measurement head without the sample.

4.3.5 Thermal properties

The thermal properties of carbon felts were studied by measuring the thermal conductivity [$Wm^{-1}K^{-1}$] and thermal resistivity [Km^2W^{-1}] of the samples using Alambeta Instrument (SENSORA, Czech Republic) according to Standard EN 31092. For each sample, the measurement was repeated five times.

4.3.6 Electrical conductivity

The volume electrical resistance R_v [Ω] of the obtained carbon felts was measured in accordance with the ASTM D257-14 standard, using an Agilent 5313A resistance meter under conditions of 55% relative humidity and 23 ℃ temperature. After conducting ten measurements on each sample using a circular electrode, the volume resistivity r_v [Ω.m] and conductivity γ [S/m] were calculated.

$$r_v = R_v \frac{S}{t} \quad (5)$$

$$\gamma = \frac{1}{r_v} \quad (6)$$

Where t [m] is the material thickness and S [m^2] is the surface area of measurement electrodes.

4.3.7 Resistive heating

The electrical heating performance of the carbon felt samples was studied by connecting samples to a power source and applying varying voltages. An infrared camera (FLIR E6, USA) was used to record the temperature of the samples, with an emissivity of 0.95 [30].

4.3.8 Filtration efficiency

The gas filtration performance of the sample was evaluated using the MPF 1000 HEPA (PALAS GmbH, Germany) filtration instrument with Dioctyl sebacate (DEHS aerosols) as the dust. To investigate the penetration of aerosol particles, a scanning mobility particle sizer was employed. The filtration efficiency was obtained from Equation (7).

$$\text{Filtration efficiency} = 1 - \frac{C_{down}}{C_{up}} \tag{7}$$

where C_{down} and C_{up} are the particle concentration in the downstream and the upstream, respectively [31].

4.3.9 EMI shielding effectiveness

EMI shielding effectiveness testing was conducted in the frequency range of 30 MHz to 3 GHz using the coaxial transmission line method, following ASTM 4935–10, designed for evaluating flat materials. Experimental apparatus included a coaxial specimen holder (EM-2107A, Electro-Metrics, Inc.) with input and output signals connected to a vector network analyzer (Rhode & Schwarz ZNC3). The analyzer was specifically configured for generating and receiving electromagnetic signals. The total EMI shielding effectiveness (SE_T) was characterized by the ratio of transmitted power to incident power and is typically presented as follow.

$$SE_T[dB] = -10\log\frac{P_T}{P_I} = SE_A + SE_R \tag{8}$$

Where P_T and P_I refer to the transmittance power and incident power, respectively. SE_A and SE_R are used to describe the shielding effectiveness resulting from absorption and reflection (including secondary reflections), respectively. They can be calculated from the total reflection (R) and transmission (T) components of the incident power, along with the scattering parameters (S_{11} and S_{21}), using Equation (9-12) [32][33] [34].

$$R = |S_{11}|^2 \tag{9}$$

$$T = |S_{21}|^2 \tag{10}$$

$$SE_R[dB] = -10\log(1 - R) \tag{11}$$

$$SE_A[dB] = -10\log(\frac{T}{1-R}) \tag{12}$$

4.3.10 Structural stability

To evaluate the structural stability of the carbon felts under different types of deformation, a custom testing method was developed. In simple terms, when the structure of a conductor undergoes physical damage, its conductive network can be partially disrupted. Leveraging this fact, the real-time monitoring of the resistance of a sample in a bent state can be used to

investigate whether its structure has been damaged. As shown in Figure 4.1, one end of the sample was fixed at point A, while the other end was clamped at point B. During the testing process, point A remained stationary, while point B rotated the sample in a circular motion. As the sample end moved from point B to point C, the sample underwent a transition from a straight state to a bent state, as depicted in Phase I and Phase II in the Figure 4.1. During the aforementioned motion process, both ends of the sample were consistently connected to an ohmmeter, and the resistance value of the sample was recorded. In the present work, one end of the sample was kept in motion at 200 rpm for 20 min. The same stability testing was also applied to the resistive heating of the carbon felt by replacing the ohmmeter with a power supply.

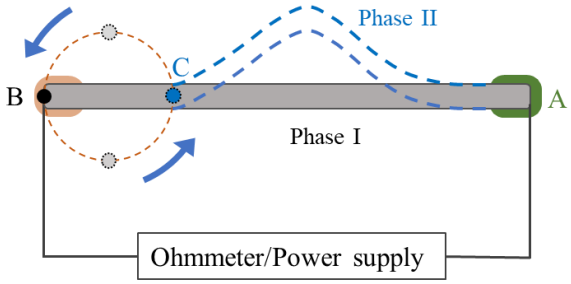

Figure 4.1 Schematic diagram of the structural stability test.

4.3.11 Raman spectra

Raman spectroscopic analysis was performed utilizing a DXR Raman microscope (Thermo Scientific, USA) equipped with an excitation laser emitting at a wavelength of 532 nm and operating at a laser power of 8.0 mW. The specimens were scrutinized under an Olympus MPlan microscope with a magnification of 50, employing a spectrograph aperture set at 50 μm. Spectral data were acquired across the range of 3500-50 cm^{-1} prior to baseline correction.

4.3.12 XRD

The crystal structure of the carbon felt was analyzed using an analytical X'Pert PRO MRD X-ray diffractometer with a Cu-Kα1 radiation source.

4.3.13 TGA

The Thermogravimetric analysis (TGA) was conducted up to 800 °C with a heating rate of 10 °C/min in an N_2 atmosphere using the TGA/SDTA851e instrument (Mettler-Toledo).

4.3.14 Antibacterial properties

To evaluate the antibacterial properties of the obtained samples, Escherichia coli strain (CCM 7395) and Staphylococcus aureus strain (CCM2446) obtained from Masaryk University in Brno were utilized. Samples sized 1×2 cm were added to 25 ml of bacterial inoculum and thoroughly homogenized by agitation. Samples were taken after homogenization at 2, 5, and 24 hours, transferred to petri dishes, and then poured with PCA agar (BioRad). Subsequently, the samples were cultured at 37°C for 48 hours. Finally, colony-forming units (CFU) were counted.

Additionally, bacterial inoculum not mixed with samples was extracted and cultured as a control.

5 Summary of the results achieved

5.1 Effect of Different Load Modes during Carbonization on the Properties of Carbon Felt

5.1.1 Effect of Different Load Modes on Sample Shrinkage.

In the preparation of flexible fibrous materials, the overall morphology of the sample is a crucial factor that cannot be overlooked. This factor is intricately linked to the structural stability and reproducibility of the resultant product. Hence, this study initiates with an examination of the shrinkage behavior of the samples under various loading conditions. Figure 5.1 and 5.2 illustrate the variations in mass, dimensions and size of the samples prepared under different loading conditions, respectively. Evidently, samples without loading exhibit significant alterations in both mass and size after carbonization. In contrast, both loading modes mitigate the shrinkage of resulting carbon samples, particularly notable at a temperature of 1000 ℃. However, the variation in thickness of the samples follows a distinct trend compared to the changes in mass and size.

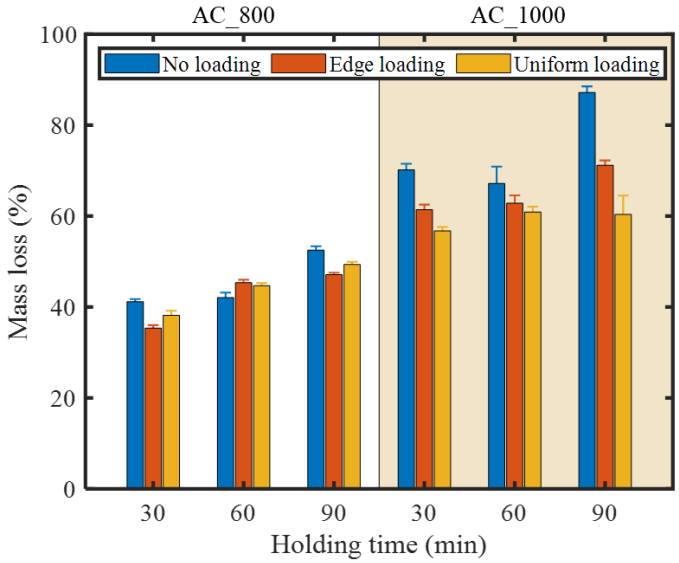

Figure 5.1 Mass loss of the obtained carbon felts under different loading modes.

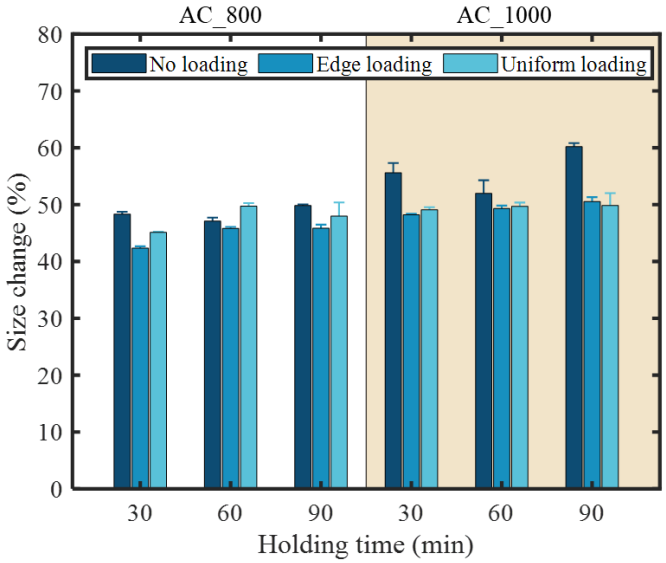

Figure 5.2 Size change of the obtained carbon felts under different loading modes.

Furthermore, photographs of the carbon felt obtained under different loading conditions are presented in the Figure 5.3. It can be observed that the unloaded sample exhibit irregular deformations after carbonization. This is attributed to the uneven shrinkage of the fibers under the heated conditions, resulting in unpredictable deformations of the fiber assembly. Such unpredictability of the visual morphological changes is unacceptable for the preparation of stable and reproducible specimens. Later, the flexibility of the samples was observed by placing the handle of a knife onto the inclined specimens. Observably, samples with no load and edge loading displayed bending when subjected to pressure, showcasing excellent flexibility, whereas samples under uniform loading appear relatively rigid. In summary, while samples with no load do exhibit favorable flexibility, they are also accompanied by shrinkage and uncontrollable product morphology. Both loading modes decelerate the shrinkage, with the edge loading mode particularly preserving the flexibility of the samples. Therefore, in terms of the morphological appearance of the obtained samples, the edge loading mode proves more conducive to achieving the desired sample characteristics.

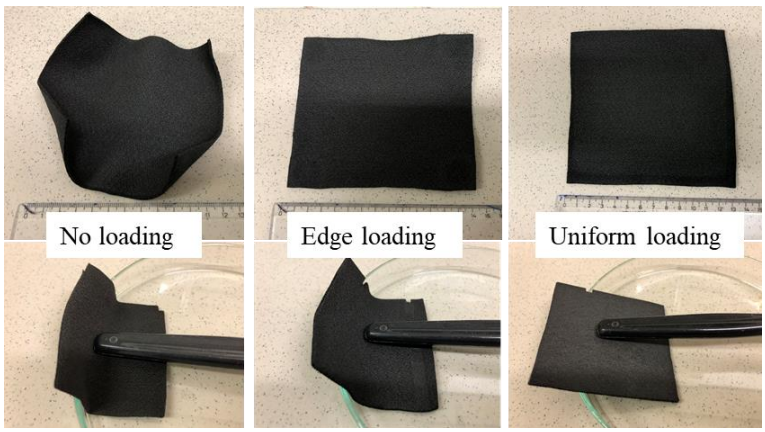

Figure 5.3 Photographs of the obtained carbon felts under different loading modes.

5.1.2 Effect of Different Load Modes on Mechanical Properties

The investigation of the mechanical properties of the obtained carbon felt is of paramount importance due to its highly porous nature. In view of the potential applications of carbon felt, this study examined the stiffness and tensile properties of the samples. The stiffness of the prepared samples under different conditions is shown in the Figure 5.4. It can be observed that across varying carbonized temperatures, the unloaded samples consistently exhibited the lowest bending moment. Compared to samples under uniform loading, significantly reduced bending moments were found on the edge loading samples. This phenomenon arises due to the inevitable occurrence of shrinkage deformation and curling during the heating process of the fibers. In contrast to samples under edge loading, fibers in uniform loaded carbon felts experience more external force confinement, thereby restricting fiber shrinkage deformation and curling. Researchers have established theoretical models to explore the effective stiffness of nonwoven fibrous webs [35]. The outcomes have revealed that the interplay of fiber stretching, fiber bending, and crosslink rotation deformation exerts a profound influence on the overall mechanical behavior of nonwoven fibrous networks. Among these, a significant reduction in the stiffness of the fibrous network was observed when the fiber curvature exceeded $\pi/3$. As a result, this observation provides a plausible explanation for the reduced stiffness found in edge-loaded samples, as they experience fewer fiber deformations and curling phenomena. Furthermore, it can be observed that longer carbonization time and higher carbonization temperatures lead to further reductions in the stiffness of the resulting samples. This is also be attributed to the influence of carbonization process parameters on the shrinkage of the fibers obtained.

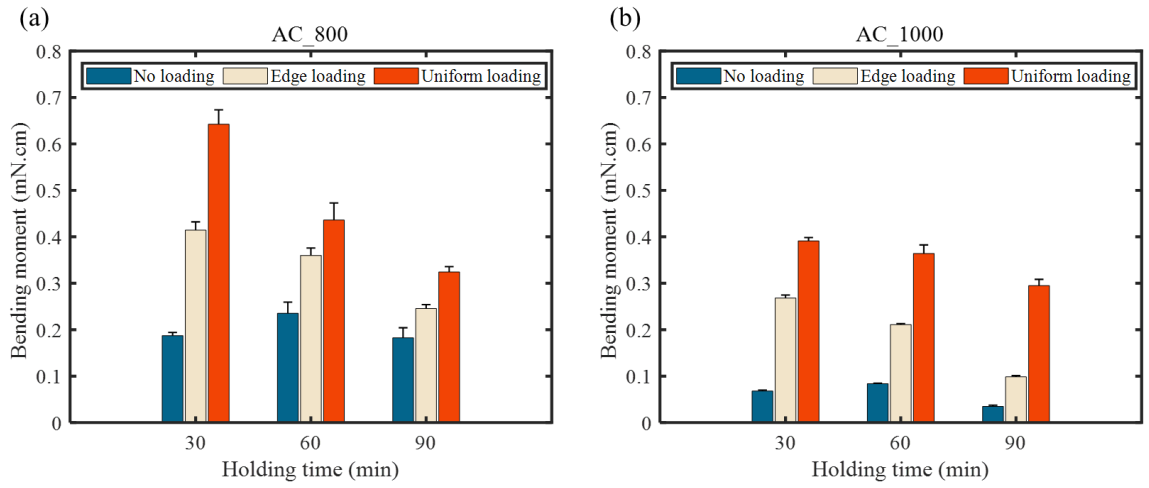

Figure 5.4 Stiffness of the obtained carbon felts under different loading modes at 800℃ (a) and 1000℃ (b).

Subsequently, the tensile properties of the samples were studied, and the breaking stress and breaking elongation of the specimens are displayed in the Figure 5.5. It is evident that the unloaded samples subjected to a holding time of 30 min exhibit the highest tensile stress, whereas

an increase in the holding time to 90 min results in the lowest tensile stress. For carbonization temperatures of 800 ℃ and 1000 ℃, the carbonization duration leads to a significant decrease in tensile stress, ranging from 0.97 MPa to 0.44 MPa and from 0.85 MPa to 0.17 MPa, respectively. On the other hand, the tensile stress of the other two loaded samples demonstrates a relatively stable behavior, remaining within the range of 0.6 MPa to 0.9 MPa regardless of the carbonization temperature and duration. In the realm of nonwoven textiles, the principal mechanism governing tensile fracture primarily involves the fracture of fibers and inter-fiber slippage. During the process of tensile loading, individual carbon fibers may undergo fracture due to external stresses, consequently leading to the overall fracture of the fiber assembly. In the carbonization process, applying tension to the fibers is widely acknowledged as an effective means of enhancing the tensile performance of carbon fibers [16]. In this study, the improved tensile properties observed in the loaded samples may be attributed to this particular factor, leading to greater stability in their tensile behavior. In the case of unloaded samples, extended carbonization adversely affects the molecular alignment within the fibers, resulting to a weakening of the mechanical properties. Furthermore, the breaking elongation results in Figure 5.5 (b) indicate that sample subjected to edge loading exhibit superior breaking elongation compared to the uniform loading sample. This is attributed to the pressure applied by uniform loading during the carbonization process, which imparts greater brittleness to the fiber assembly. In samples subjected to edge loading, the majority of fibers remain unexposed to direct compressive forces during the preparation process, leading to the development of carbon felt with enhanced elasticity and flexibility.

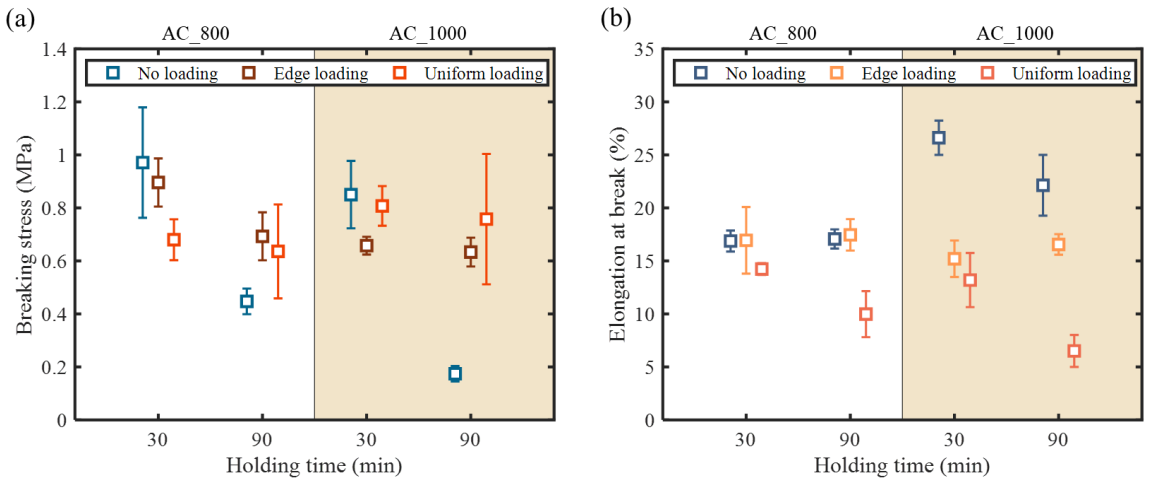

Figure 5.5 Breaking stress (a) and elongation (b) of the obtained carbon felts under different loading modes.

5.1.3 Effect of Different Load Modes on Thermal Properties

Understanding the thermal transport performance of carbon felts is crucial for numerous engineering applications. By modulating thermal conductivity, materials can be designed to meet specific thermal management requirements in various applications, such as heat dissipation in

electronic devices. Thermal conductivity, measured as the rate at which heat is transferred through a material per unit area and unit thickness under a specified temperature gradient, is an intrinsic property of materials. As depicted in Figure 5.6 (a), it is observed that among the samples prepared using three different loading modes, the thermal conductivity is highest for the edge-loaded sample, followed by the uniform loaded sample, with the unloaded sample having the lowest thermal conductivity. (Major influence has pore size and their amount) The thermal conduction in carbon fibers primarily occurs through lattice vibrations. Within the lattice, carbon atoms oscillate around their equilibrium positions, generating phonons (lattice vibrational quanta). These phonons propagate within the lattice, carrying thermal energy [36]. It has been found that the thermal conductivity of carbon fibers gradually increases asymptotically with the enhanced preferential orientation degree of the crystalline segments within the fibers [37]. During the carbon felt preparation process, edge loading provides the fibers with the appropriate tension, optimizing the preferred orientation of the internal crystalline phases within the fibers, thereby enhancing the overall thermal conductivity of the fiber assembly but porosity effect is more important. With the increase in carbonization temperature from 800 ℃ to 1000 ℃, there is an observed elevation in the thermal conductivity of the samples. This phenomenon can be attributed to the enhanced interatomic bonding among carbon atoms at higher carbonization temperatures, thereby leading to an improvement in material crystallinity. Greater crystallinity is conventionally correlated with superior thermal conductivity, as it facilitates more efficient heat transfer between crystalline regions. Thermal resistance is determined by both the thermal conductivity and thickness of the material, and it serves as an indicator of the ability to impede the flow of heat through a unit area of the material. From Figure 5.6 (b), it can be observed that the thermal resistance of the unloaded sample is almost 40% higher than that of the loaded samples, while the difference in thermal resistance between the two loaded samples is not as significant as the difference in thermal conductivity. This is primarily attributed to the varying thicknesses of the samples under different loading modes, as demonstrated in the previous section. Generally, the thermal properties of the samples, reveals that the edge loading mode enhances the thermal conductivity of the samples by optimizing the orientation of internal crystalline phases within the fibers and changing real porosity.

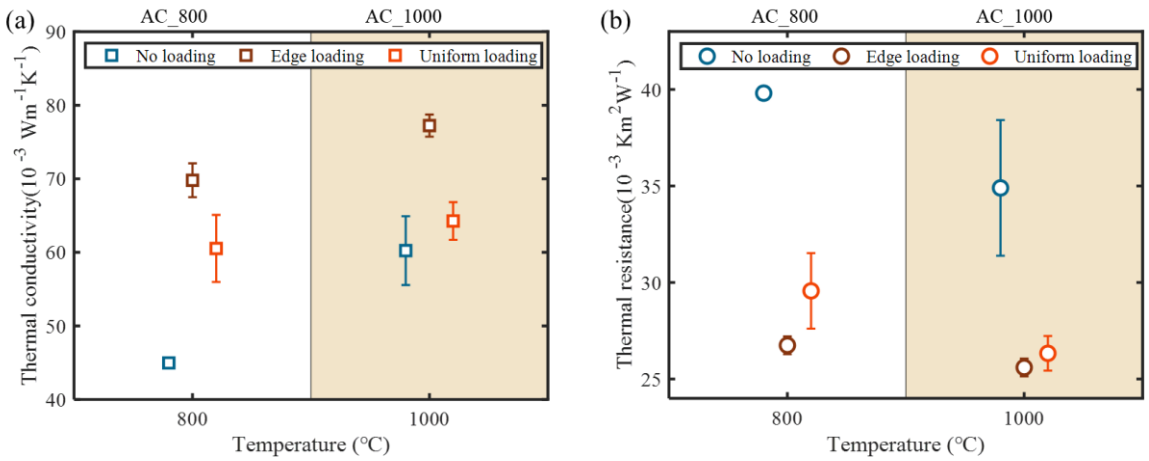

Figure 5.6 Thermal conductivity (a) and resistivity (b) of the obtained carbon felts under different loading modes

5.1.4 Effect of Different Load Modes on Electrical Properties

The volume electrical conductivity of carbon felt samples obtained under different loading conditions in this study is presented in the Figure 5.7. At a carbonization temperature of 800 ℃, the samples exhibited relatively lower electrical conductivity, with no significant differences among different loading modes. As the temperature increased to 1000 ℃, it was observed that the edge-loaded samples exhibited the highest electrical conductivity. As mentioned earlier, edge loading provides the fibers with the appropriate tension, thereby ensuring a more homogeneous electrical connection within the fiber assembly. However, it should be noted that, when the carbonization time was extended to 90 minutes, there was a sharp decrease in the electrical conductivity of the samples. This could be attributed to the prolonged carbonization time causing damage to the fibers, consequently disrupting the internal conductive pathways within the carbon felt and reduction of porosity.

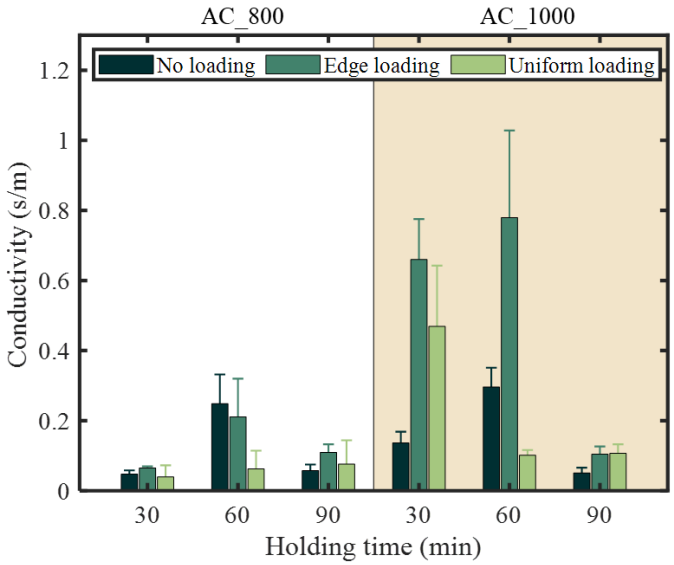

Figure 5.7 Electrical conductivity of the obtained carbon felts under different loading modes

5.2 Effect of PTFE Coating on the Properties of Carbon Felt

As an industrial dust filter felt, the surface is typically treated with hydrophobic treatments to improve applicability. In this thesis, one side of the acrylic-based felt was coated with PTFE, with a mass content of approximately 0.5% of the total felt weight. One of the challenges in processing waste textiles is the mixture of various fibers, due to the lack of efficient methods for separating different fibers. For pyrolyzed fiber waste, such mixed fibers or fiber coatings may introduce uncertainties in the performance of the resulting carbon materials. We investigated the effects of a PTFE coating on the properties of acrylic-based carbon felt. Since the raw material had PTFE coating only on one side and was very thin, its impact on acrylic fibers during pyrolysis may have been minimized. Therefore, we coated the raw material with a PTFE dispersion to form a PTFE layer on the fiber surface, followed by sequential stabilization and carbonization, to examine its impact on the properties of the resulting carbon felt.

5.2.1 Effect of PTFE Coating on Sample Shrinkage and Morphology

Photographs of the samples obtained after carbonization of acrylic-based felt with PTFE coatings of different concentrations are shown in Figure 5.8(a). It can be clearly observed that the size of the samples increases with the concentration of the PTFE coating. Notably, when the PTFE concentration reaches 30% and 60%, the change in sample size becomes more pronounced. The quantified results of the changes in sample mass and size are shown in Figure 5.8(b). The loss in sample mass did not change significantly in the range of low concentration PTFE coatings (0%–12%). When PTFE reached 30%, a notable decrease in mass loss was observed, which further decreased as the concentration increased to 60%. This indicated that mass loss in the carbon felt was only reduced when the PTFE coating fully enveloped the fibers. In contrast, the changes in sample size followed the variations in PTFE concentration, decreasing accordingly. Notably, when PTFE concentrations were increased to 30% and 60%, the decrease in sample size changes became more pronounced. As PTFE concentration increased, the change in sample size exhibited a different trend compared to mass loss. This may be due to the initially high porosity of the felt, where higher PTFE concentrations not only enveloped the fiber surfaces but also filled the gaps between the fibers. The filling of the original gaps between fibers with PTFE inhibited the heat-induced shrinkage of the acrylic felt, resulting in a significant difference in the variation of sample size.

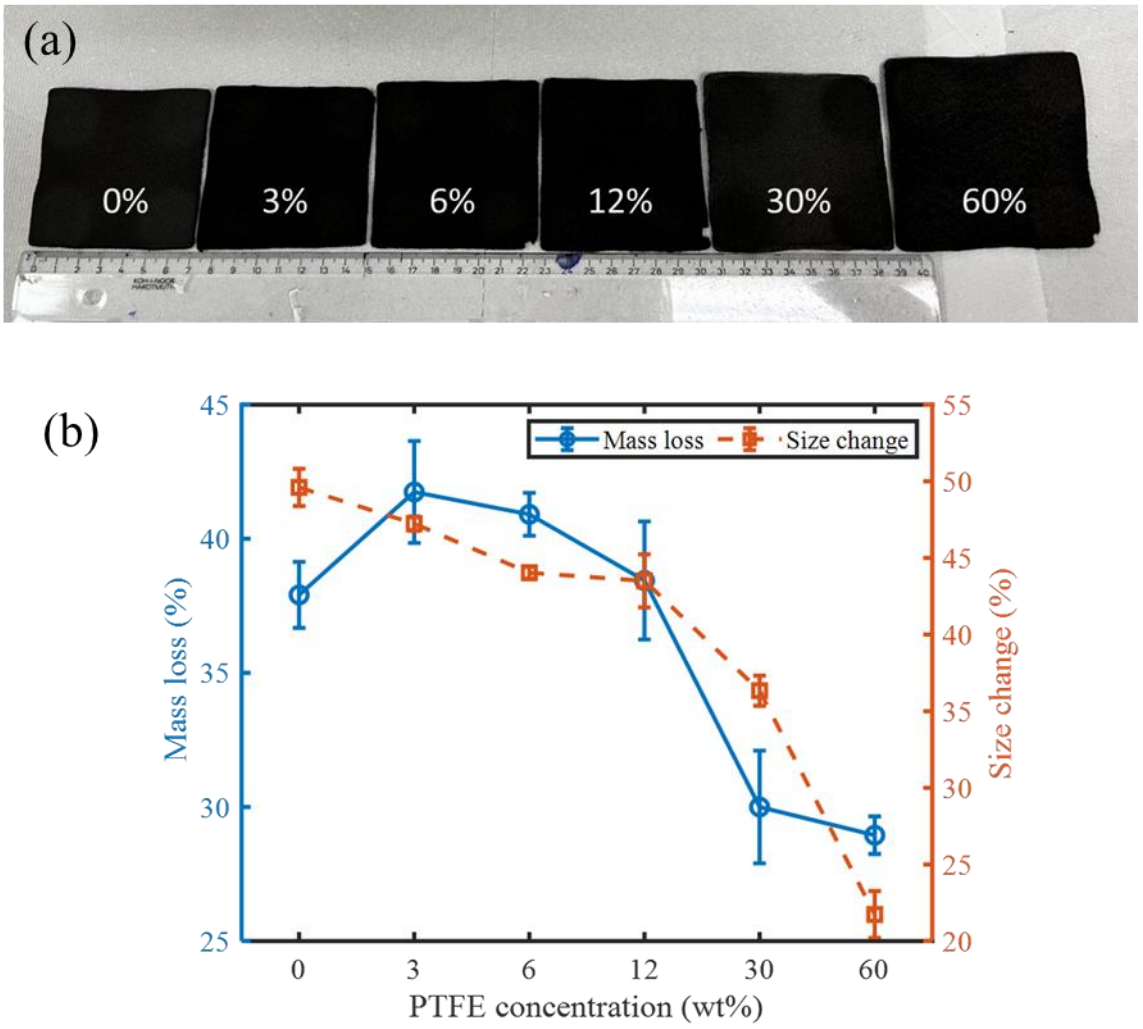

Figure 5.8 Shrinkage of the carbon felts obtained with different concentration PTFE coating. (a) Photographs of the samples. (b) Mass loss and size change.

To further investigate the effect of PTFE on acrylic-based felt during pyrolysis, we conducted TGA on the samples, and the results are shown in Figure 5.9. The thermal decomposition of exposed acrylic fibers mainly occurred between 300°C and 500°C. However, the decomposition of pure PTFE occurred around 600°C. Therefore, within the range of 300°C to 500°C, the surface of the fibers remained enveloped by an undecomposed PTFE layer, hindering the release of gaseous products produced during the pyrolysis of acrylic. This could be the reason for the reduction in mass loss in samples with high PTFE coating concentrations. Additionally, during the acrylic decomposition stage, the undecomposed PTFE between the fibers acted as a support structure, maintaining the original structure of the felt and slowing down changes in sample size.

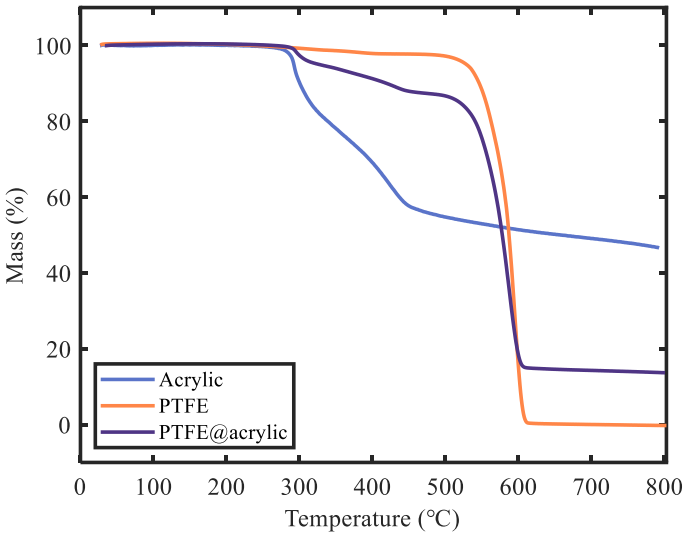

Figure 5.9 TGA curves of the acrylic-base felt, PTFE, and PTFE coated felt.

5.2.2 Effect of PTFE Coating on Sample Mechanical properties

The stiffness of the samples prepared under different PTFE concentration conditions is shown in Figure 5.10. It can be observed that within the low concentration range of 0%–12%, the samples exhibited similarly low bending forces with almost no differences. When PTFE concentrations were increased to 30% and 60%, the bending forces of samples significantly increased and correlated positively with concentration. This phenomenon is due to the fibers' inability to deform during pyrolysis, because of the adhesive effects of PTFE between the fibers. As mentioned above, the overall mechanical behavior of the nonwoven fiber network is influenced by the interplay of fiber stretching, fiber bending, and cross-link rotation deformations. Evidently, the solid PTFE filling between the fibers hindered fiber curling and cross-link rotation during pyrolysis, resulting in increased stiffness of the obtained carbon felt.

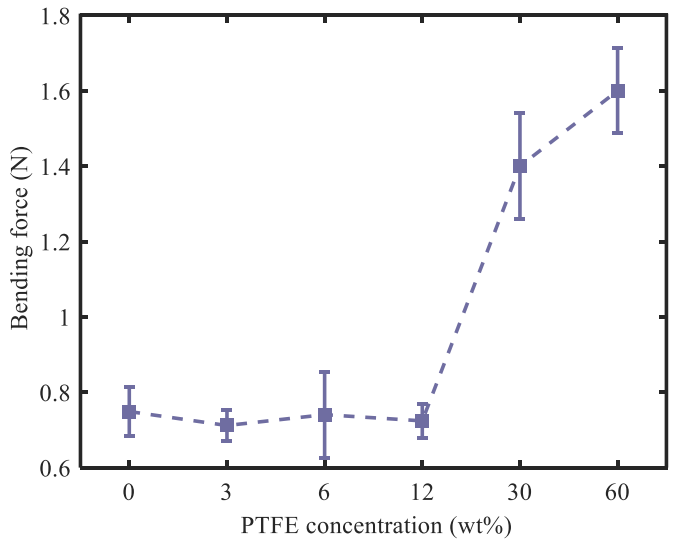

Figure 5.10 Stiffness of the carbon felts obtained with different concentration PTFE coating.

The tensile strength and modulus of the samples are shown in Figure 5.11. In comparison to

uncoated samples, low PTFE concentrations of 3%–12% resulted in lower tensile strength. When concentrations increased to 30% and 60%, the tensile strength was slightly higher than that of the uncoated samples. The enhancement of the samples' modulus due to the coating was more pronounced. Low PTFE concentrations modestly increased the modulus by about 10 MPa, whereas high concentrations significantly increased the modulus, from 15 MPa to 76.4 MPa. Such a marked increase in modulus can be attributed to the control exerted by PTFE on fiber deformation during pyrolysis, as discussed in the previous section, which led to increased stiffness in the carbon felt samples. However, since PTFE was mostly converted into gaseous products after carbonization, it did not significantly improve the tensile strength of the samples.

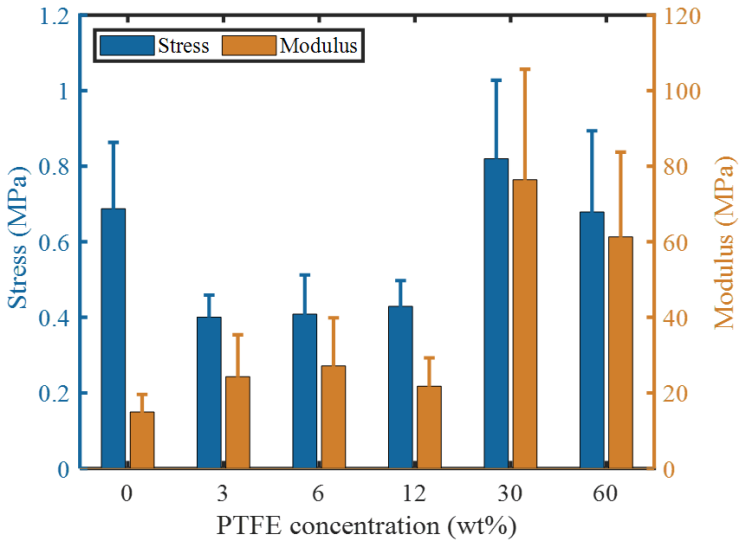

Figure 5.11 Tensile properties of the carbon felts obtained with different concentration PTFE coating.

5.3 Flexible carbon felt characterization and properties.

After exploring the process during carbonization, we established the optimal process for preparing flexible conductive carbon felt. In this section, the carbon felt prepared using the edge-loading mode was characterized, and its EMI shielding and resistive heating properties were studied.

5.3.1 Morphology and Structure Characterization

The SEM images of the carbon felts obtained are illustrated in Figure 5.12. The carbon fibers obtained from the acrylic-based precursors underwent a change in their fineness, exhibiting a finer structure with increasing carbonization temperature. This transformation can be attributed to the depletion of hydrogen and nitrogen in acrylic as the degree of carbonization escalated, resulting in fiber shrinkage. Moreover, when carbonized at 1100℃, the carbon fibers displayed prominent wrinkles on their surface. Wrinkles on the surface of fibers can serve several advantageous purposes in material science. Firstly, they contribute to an increase in the overall

surface area of the fiber, which in turn enhances processes such as adsorption, absorption, and exchange. Secondly, these wrinkles also bolster the strength and rigidity of the fibrous material, rendering it better suited to withstand external forces and pressures. Furthermore, the presence of microscale indentations and protrusions on the fiber surface aids in improving adhesion.

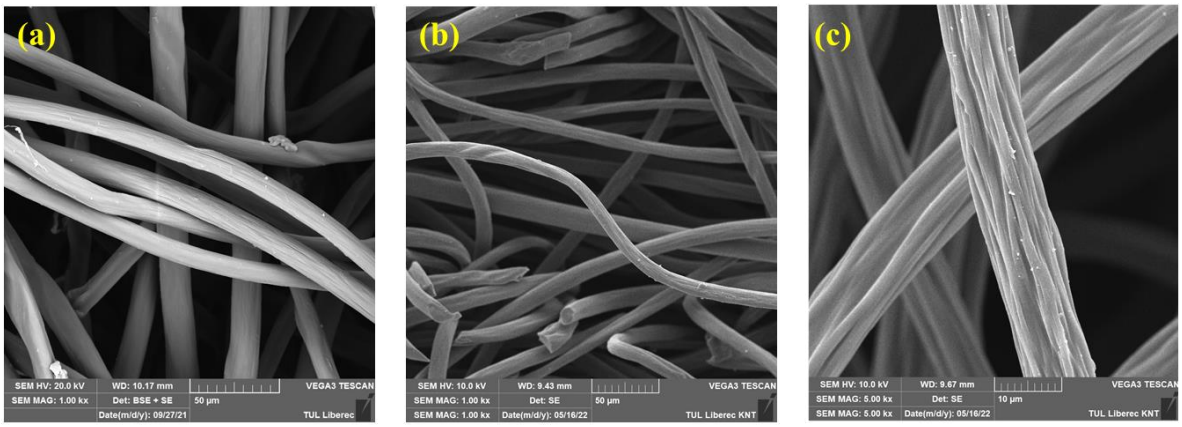

Figure 5.12. Fiber morphology of the carbon felts. SEM images of precursor acrylic fiber(a), AC_800(b), and AC_1100(c).

The Raman spectrum of the obtained carbon felt is depicted in Figure 5.13. Typically, the D band at 1350 cm^{-1} is attributed to defects and disordered carbon structure, while the G band at 1580 cm^{-1} is induced by the sp^2 hybridization of carbon. The peak intensity ratio of the D band to the G band (I_D/I_G) is considered to be linearly correlated with the inverse of the in-plane crystal size. Thus, this indicator can be utilized to quantify the amount of ordered graphite structure [38]. After fitting the obtained spectra with a Gaussian function, the I_D/I_G ratio of the resulting samples decreased from 1.45 to 1.05 as the carbonization temperature increased from 800 ℃ to 1000 ℃. This indicates that due to the removal of non-carbon elements such as oxygen and a reduction in the number of defects, the carbon structure within the fibers is transitioning from a mixed-bonded amorphous carbon to a predominantly sp^2-bonded carbon [40].

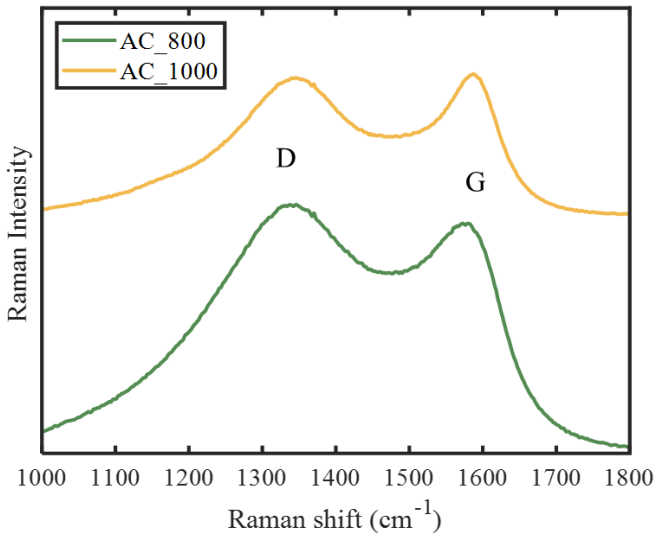

Figure 5.13 Raman spectrum of the carbon felts.

5.3.2 EMI shielding behavior

Figure 5.14 illustrates the EMI shielding effectiveness (SE) of a single-layer carbon felt in the frequency range from 30 MHz to 3 GHz. It is clear that the total SE increases with the rise in carbonization temperature. As the carbonization temperature increases from 800 to 1100 ℃, the EMI SE significantly rose from 17-20 dB to 42-57 dB. In accordance with the general requirements for EMI SE in textile materials, all samples in this study, with the exception of AC_800, demonstrated an "excellent" rating. AC_800 was characterized as "very good"[39].

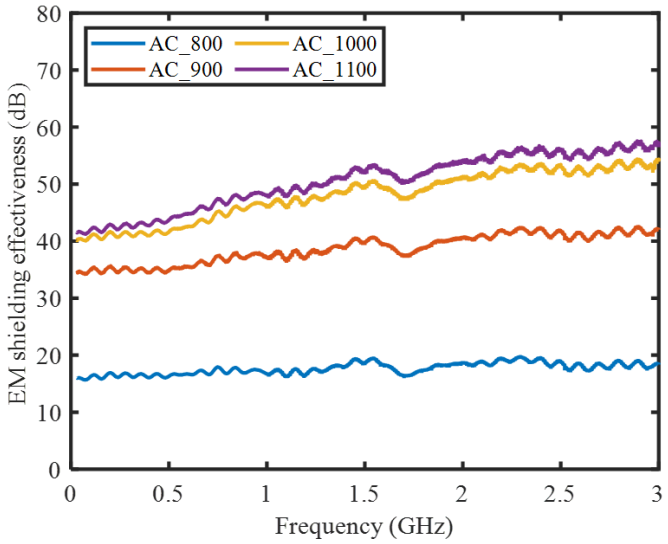

Figure 5.14 Total EMI shielding effectiveness from 30MHz to 3GHz of the carbon felts.

When designing EMI shielding materials, light weight and thickness should also be considered. Therefore, we adopted the concept of a specific SE value (divide the SE_T by the density and thickness of the material) to compare the shielding performance of materials in a more comprehensive way [41]. Figure 5.15 compares the specific SE values of this work with those reported in other literatures. Due to the low density of the carbon fibers, the high porosity of the carbon felts and the remarkable SE_T, the specific SE values of the carbon felts sample AC_1000 and AC_1100 in this work outstandingly outperform the other reported materials, including carbon nanotube [42][43], graphene [44][45][46], carbon black [43], carbon foam [47], carbon nanofiber mat [32], metal foam [48], and MXene [41].

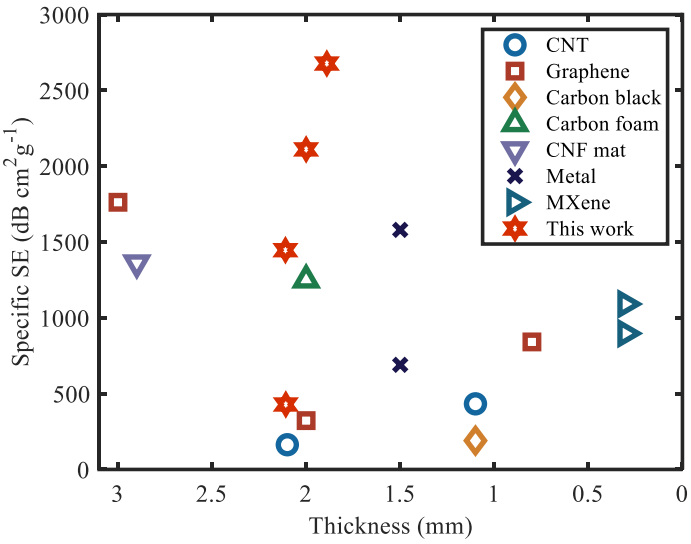

Figure 5.15 Comparison of the specific SE as a function of the thickness

In summary, the prepared carbon felt exhibits excellent EMI shielding performance and, due to its flexibility and lightweight nature, has great potential for a wide range of applications.

5.3.3 Electrical Resistive Heating Performance

The varying response of different samples to different applied voltages is shown in Figure 5.16. The temperature rose as the voltage increased, in accordance with Joule's Law. Among them, the sample AC_1100 reached a high temperature of nearly 200 ℃ at a 3 V and 0.9 A, indicating that this sample exhibited a responsive and broad range of temperatures for heating under voltage. Under the same applied voltage, the heat generation temperature increased with the elevation of carbonization temperature. This phenomenon can be attributed to the higher electrical conductivity of the sample, as previously described. The graphite layers inside the carbon felt had an irregular arrangement, and the higher graphitization promoted the formation of a dense conductive network in the structure. When a voltage was applied, the graphite layer heated up due to Joule heating. At this point, the graphite layer acquired vibrational energy and diffused the thermal energy in a common vibrational mode throughout the system, raising the temperature of the sample [9]. The heat was then transferred to the surroundings by conduction or radiation, resulting in an increase in the surrounding temperature.

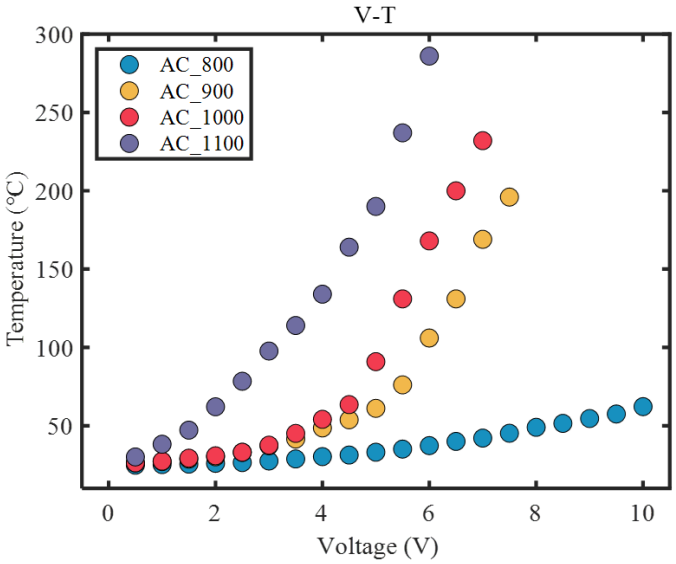

Figure 5.16 Changes of heating temperature of carbon felts as functions of the applied voltage.

Additionally, the relationship between power and temperature was analyzed, as shown in Figure 5.17. From the power-temperature curves of different samples, it can be observed that as the carbonization temperature increased, the slope became steeper. In other words, at the same power level, samples with higher carbonization temperatures can achieve higher resistive heating temperatures. This suggests that the electrical energy efficiency of the samples can be adjusted through parameters in the preparation process. Heating efficiency is a key parameter for evaluating the performance of electric heaters and is defined as the ratio of temperature rise per unit area to input power. The heating efficiencies of samples AC_900, AC_1000, AC_1100 in this work were calculated to be 204.4, 195.2, and 448.6 °C W^{-1} cm^2, respectively. Such high heating efficiencies have surpassed many others reported using higher cost conductive materials such as nanosilver [49], carbon nanotubes [50], graphene [51], and MXene [52].

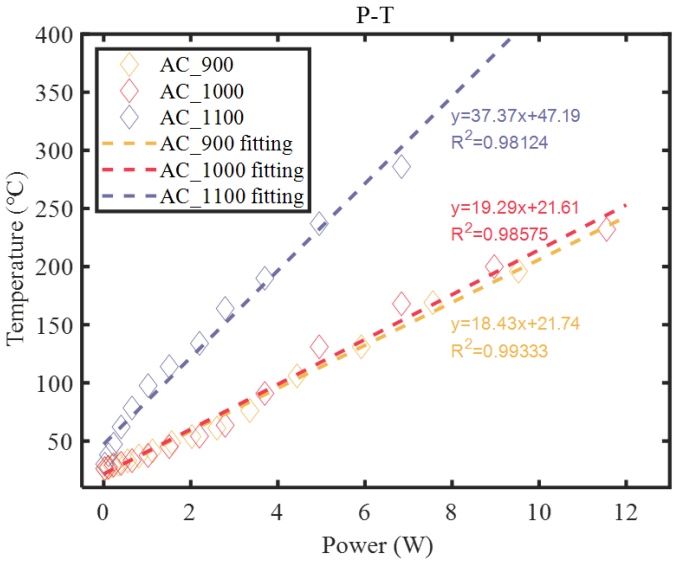

Figure 5.17 Changes of heating temperature of carbon felts as functions of electric power.

Later, the heating and cooling behavior of the samples was investigated by applying a constant

voltage (Figure 5.18). Considering that voltages in the range of 3-5V are more readily available in everyday life (from batteries, USB chargers, etc.), this study conducted heating experiments on the samples using 3V and 5V voltages. Under these voltage conditions, the AC_800 sample exhibited suboptimal heating performance, with a maximum temperature of only 35 ℃ reached. In contrast, the other two samples showed a significant increase in heating rate and reached much higher maximum temperatures. However, due to the thickness of the samples, it takes a considerable amount of time for the temperature to return to the initial temperature after the power was disconnected. These properties make the samples suitable for applications with different temperature requirements, such as lower temperature for body temperature management, and higher temperature for sterilization and anti-icing.

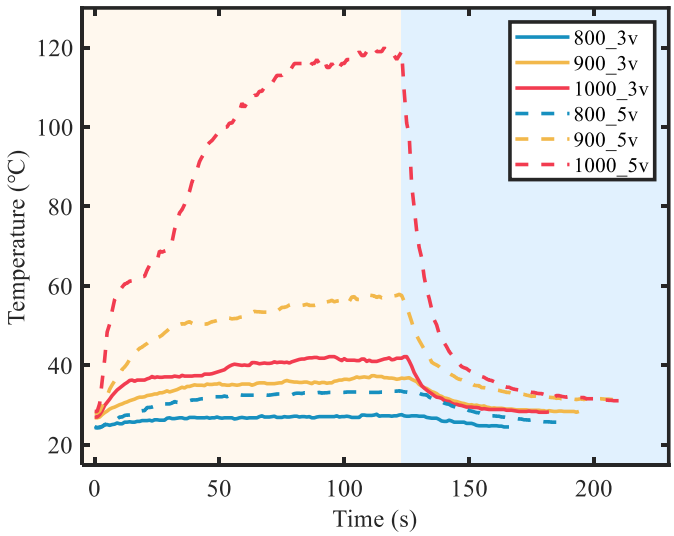

Figure 5.18 The time-temperature curve under a voltage of 3V and 5V.

5.3.4 Structural Stability

We examined the change in resistance and resistive heating performance of the samples throughout in-situ testing during dynamic bending processes to assess their structural stability. Figure 5.19 illustrates the variation in sample resistance with bending cycles. The resistances of AC_900, 1000, and 1100 samples remained stable within 4000 bending cycles, showing minimal decline. This demonstrated their remarkable structural stability under repeated bending. This can be attributed to the reduced brittleness of the internal fibers and the overall good flexibility of the carbon felt, where the bending deformation applied was not sufficient to cause fiber breakage. However, the AC_800 sample exhibited an initial increase in resistance during the first few bending cycles, followed by stabilization. This is consistent with the lower carbonization temperature leading to higher stiffness mentioned in the mechanical properties section above.

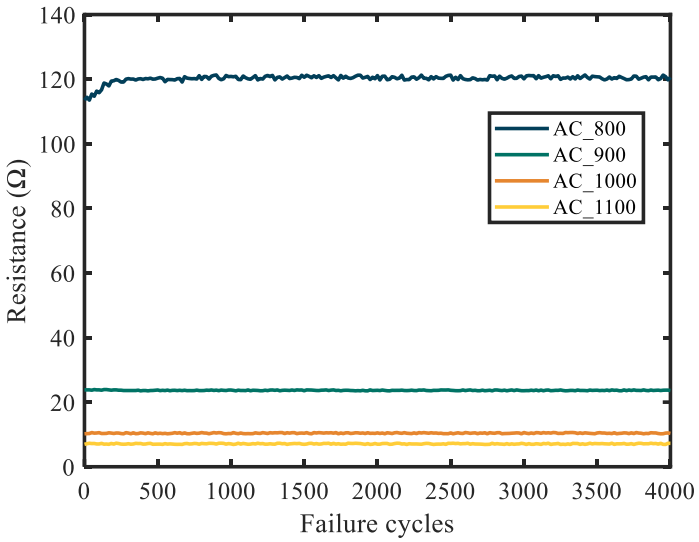

Figure 5.19 The variation of sample resistance with the number of bending cycles.

Using the same equipment, resistive heating behaviors of the carbon felt during the bending cycle was also recorded and shown in Figure 5.20. The two selected samples both exhibited stable temperatures within 1000 bending cycles at different applied voltages. This demonstrates that even under heating conditions, the sample maintained the same stability of its conductive network as at room temperature. This examination provides support for the potential application of carbon felts to deformable heaters in motion.

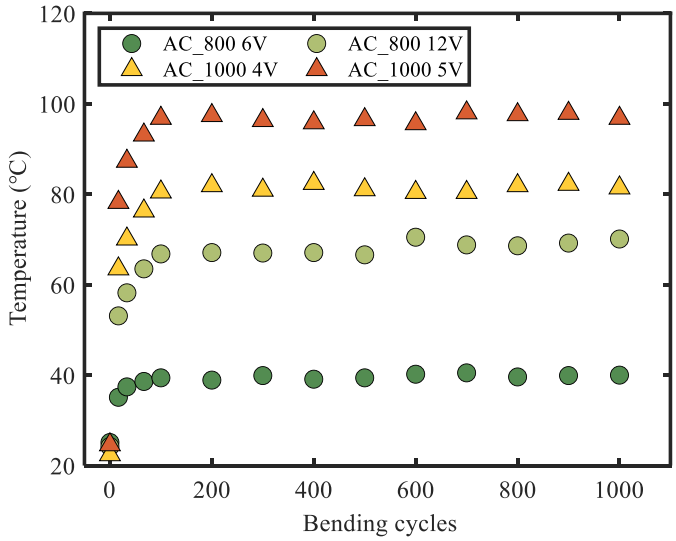

Figure 5.20 The variation of heating performance with the number of bending cycles.

5.5 Special Application of the Prepared Carbon Felt

As a flexible 3D conductive network, the manufactured carbon felt can be utilized not only for traditional conductor applications such as EMI shielding and electric heating but also as a respirator filter layer, taking advantage of the filtration properties of its raw materials. This part will explore the performance of carbon felt in this context, focusing on its suitability for use as a respirator filter layer.

5.5.1 Air Permeability and Breathability

As a potential respiratory filter material, the permeability and breathability of carbon felt need to be studied. Figure 5.21 shows the air permeability of the carbon felt at different pressures. It is clear that the permeability correlated positively with pressure and carbonization temperature. The previous results of fiber fineness distribution can well explain the phenomenon that the permeability increased with the carbonization temperature. The decrease in fiber fineness has created more space within the fiber assembly, which facilitated the air flow and thereby improved air permeability. Additionally, linear regression was performed on permeability and pressure data. The results indicate that for all samples, the R^2 values of the linear regression fits were greater than 0.99. The R^2 value of 0.99 in our linear regression analysis signifies a strong linear correlation between permeability and pressure across all samples. Furthermore, the elevated R^2 value underscores the predictive capacity of the model, indicating its effectiveness in forecasting future data points.

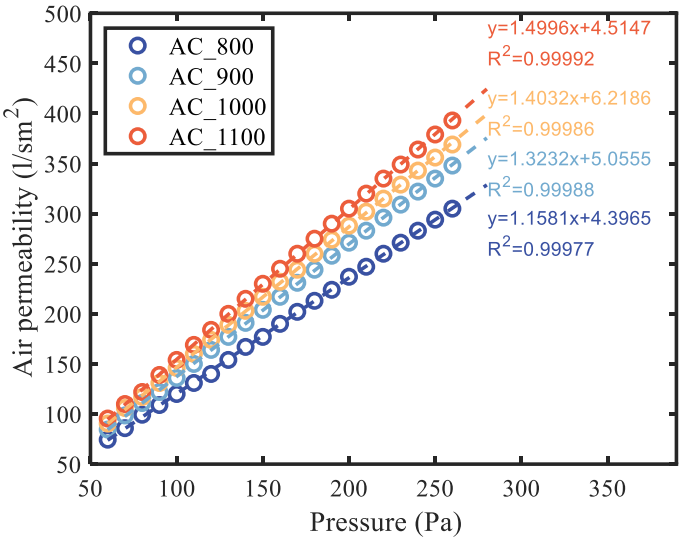

Figure 5.21 Air permeability of the carbon felts

Based on the good linear correlation between permeability and pressure, breathability was calculated through the permeability and precise respiratory filter area. The area of respiratory filter in this work is 35cm^2. First, with the determination of the filter area, the volume of air per minute that can pass through the filter media at different pressures can be obtained. Subsequently, a linear relationship between air permeability and pressure can be established. By using this linear relationship, we can assume the pressure required to achieve different air flows. The resulting breathability properties are listed in Table 5.1. Here, we assume that 100 Pa is critical value for breathing, which means that it can breathe smoothly when the value is below 100 Pa. From the data in the table, it can be noted that the samples AC_800 and 900 can satisfy the peace and walk human activity. While samples AC_1000 and 1100 can further ensure unhindered breathing

during accelerated movement. In settings such as hospitals and virus laboratories, where respiratory filters are worn, the primary physiological activities of the wearer involve sitting and walking. Hence, the carbon felts prepared in this study can all ensure respiratory performance that accommodates essential human activities.

Table 5.1 Breathability (Pa) of the carbon felts.

Air volume during various human activities	**AC_800**	**AC_900**	**AC_1000**	**AC_1100**
Peace 8 – 10 l/min	32-40	28-35	27-33	25-31
Walk 15 – 20 l/min	60-81	53-70	50-66	47-62
Accelerated movement 20 – 30 l/min	81-121	70-106	66-99	62-94
Medium work 30 – 40 l/min	121-161	106-141	99-133	94-125
Hard work 40 – 50 l/min	161-201	141-176	133-166	125-156
Extreme stress 50 – 120 l/min	201-483	176-423	166-398	156-375

5.5.2 Filtration Efficiency

After studying the permeability, the gas filtration performance was examined to assess their potential suitability for respiratory filter applications. The filtration efficiency of carbon felt samples for particles of different sizes is shown in Figure 5.22. It can be observed that for particles with a diameter less than 1 μm, the filtration efficiency of all samples was relatively low, below 50%. With the increase in particle size, there was a noticeable improvement in the filtration efficiency of all the samples. At the same time, the filtration efficiency was found to be positively influenced by the carbonization temperature. The AC_1100 sample, in particular, achieves a filtration efficiency of 93.8% for particles with a size of 1.8 μm. This is because the increase in carbonization temperature led to a reduction in fiber diameter and the formation of wrinkles on the fiber surface. These two factors synergistically increased the fiber surface area and the porosity of the carbon felt.

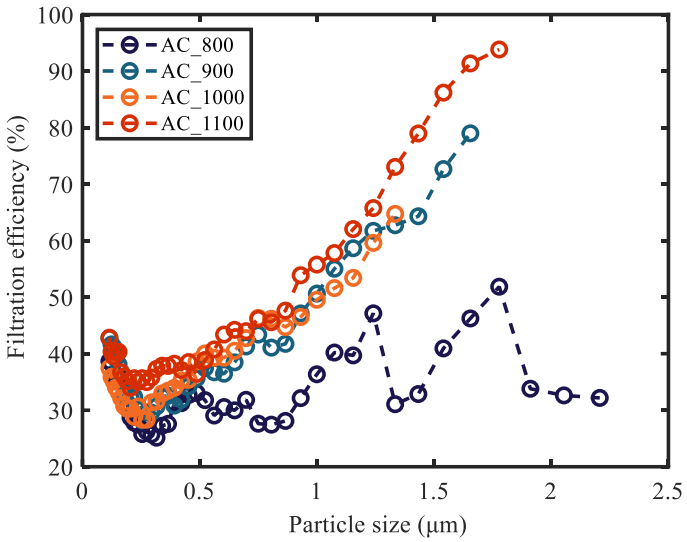

Figure 5.22 Filtration efficiency of the carbon felts.

5.5.3 Resistive Heating for Disinfection

After filtration, viruses may remain viable within the filter layer for a period of time. If left unaddressed during this period, they continue to pose a potential health hazard to the users of respiratory filters. Hence, it is imperative to promptly disinfect the respiratory filter layer. Among the disinfection methods, high-temperature treatment stands out as an effective and reliable approach. Here, carbon felt not only serves as a filtration layer but also functions as an electric heater due to its excellent electrical conductivity. In prior section the resistance heating performance of carbon felts have been studied. When the carbon felt serves as a filtration layer, it needs to be integrated into respirators. Therefore, this study first investigated the influence of different electrode configurations on the thermal distribution of carbon felts embedded within respirator. Upon determining the optimal electrode configuration, the heating behavior under electrical current was further examined.

Typically, during resistive heating processes, electrodes are positioned in parallel on either side of the sample to achieve uniform heat distribution. However, in this study, the respirator design was circular. Therefore, we experimented with various electrode configurations to ensure both feasibility within the respirator and uniform heat distribution across the sample. The three different electrode connection methods are illustrated in Figure 5.23. From the infrared image, it can be observed that when the electrodes were connected to the sample in a circumferential (I) or point (II) manner, significant localized heating occurred in the vicinity of the electrodes. When the electrodes were connected in an arc shape (III), the heat distribution in the carbon felt was relatively uniform. Therefore, symmetrically arc-shaped electrodes were designed and positioned within the respirator, and subsequent experiments were conducted using this configuration.

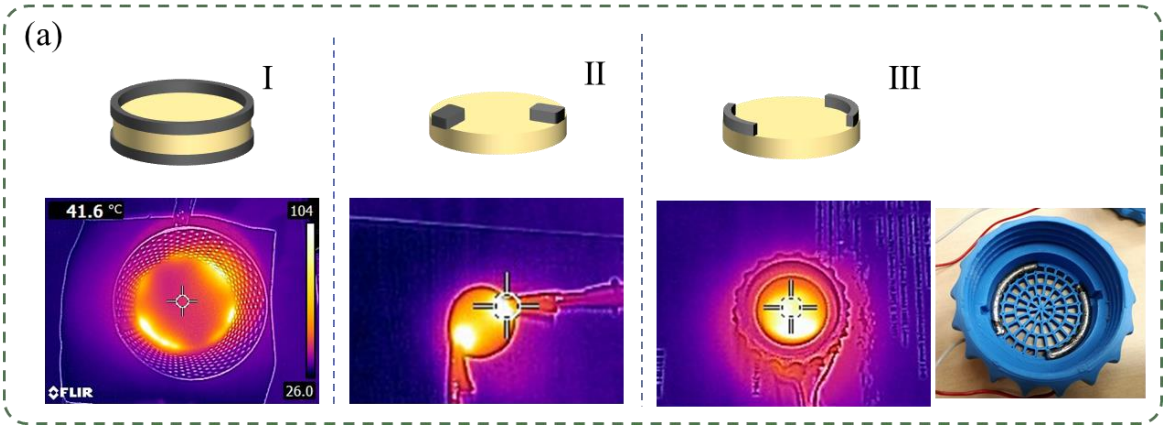

Figure 5.23 Different electrode configurations with carbon felt and their corresponding electrical heating distribution.

The heating and cooling performance of the carbon felt under constant voltage was studied to ascertain its potential for achieving disinfection purposes in practical applications. Based on safety and practical feasibility considerations, a voltage of 3V was selected for testing. The time-temperature curve is depicted in Figure 5.24. After applying voltage, the temperature of the samples rapidly increased and stabilized upon reaching a steady-state temperature. The steady-state temperatures of the four samples were approximately 45°C, 80°C, 105°C, and 188°C, respectively. Subsequently, the power supply was disconnected, and the temperature of the samples decreased. However, samples with higher steady-state temperatures did not reach room temperature within 120 seconds, as the thickness of the samples and being placed inside the respirator hindered heat dissipation. Some studies have provided recommendations for thermal inactivation of coronaviruses. Taking the example of the COVID-19, they suggested that virus inactivation can be achieved at temperatures of above 75 °C for 3 minutes, above 65 °C for 5 minutes, or above 60 °C for 20 minutes [53]. Hence, it can be stated that samples with carbonization temperatures exceeding 900°C in this study exhibited resistive heating characteristics capable of virus inactivation under low voltage of 3 V.

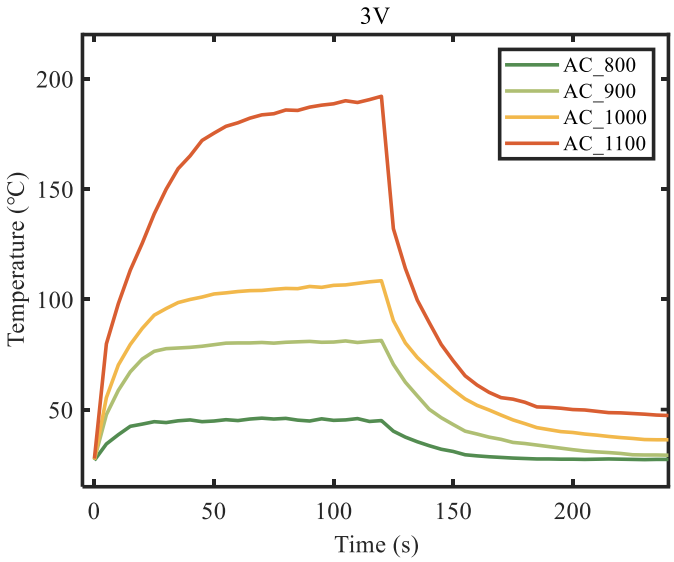

Figure 5.24 Time-temperature curve of carbon felts for disinfection.

In summary, the exceptional electrical conductivity of carbon felt enables its use not only as a respirator filter layer but also for high-temperature electric heating and sterilization. Its breathability and permeability ensure comfort when used as a respirator filter layer. Filtration efficiency testing results indicate that carbon felt achieves over 90% efficiency in filtering inhalable particles.

6 Conclusion

In this work, carbon felt was first prepared using waste acrylic-based felt as a precursor through controlled pyrolysis. The effects of different loading conditions on raw materials during the pyrolysis process on the shrinkage rate, mechanical properties, and electrical properties of the resulting carbon felt were studied. The results showed that applying edge load to the sample during the carbonization stage helps reduce the shrinkage rate of the final product, thereby allowing the carbon felt to gain flexibility and form a well-constructed conductive network. To investigate the impact of PTFE coating on the pyrolysis of acrylic-based felt, acrylic-based felt was coated with different concentrations of PTFE and subsequently subjected to pyrolysis. By examining the morphology, mechanical properties, and electrical properties of the PTFE-coated samples, we found that higher coating concentrations had a greater impact on the performance of the resulting carbon felt. Although high coating concentrations increased the modulus and electrical conductivity of the material, they also led to a loss of flexibility in the carbon felt, potentially severely limiting its application scope. Thus, it can be considered that a thin PTFE layer on one side of the raw material has a negligible impact on the shrinkage and mechanical properties of the carbon felt.

By characterizing the morphology and structure of carbon felts prepared at different carbonization temperatures under the edge load mode, it was found that as the carbonization temperature increased, the fibers became finer and wrinkled, and the porosity of the carbon felt increased. Additionally, high temperatures facilitated higher crystallinity within the fibers and the formation of an ordered graphite structure. The resulting carbon felt achieved a high EMI shielding effectiveness of 55 dB and a specific shielding effectiveness value of 2676.9 $dBcm^2g^{-1}$ due to the formation of a dense, highly conductive network and high porosity. Additionally, the carbon felt demonstrated excellent heating efficiency and high heating rates in resistive heating tests. Finally, structural stability was studied through a self-designed experiment. The results indicated that the carbon felt could maintain internal conductive pathway stability through multiple bending cycles even under heating conditions. The flexible carbon felt, with its lower manufacturing cost, good chemical and structural stability, and breathability, shows potential for a wide range of applications in wearable heaters, flexible EMI shielding, and other related fields. This work also investigated the feasibility of converting acrylic-based filter felts into carbon felts for use in respiratory filtration layers. The excellent electrical conductivity of carbon felt allows it to be used not only as a respiratory filtration layer but also for high-temperature electrical disinfection. The design of the mask body and corresponding electrode configuration enabled controlled resistive heating performance, ensuring the reliability of high-temperature disinfection of the carbon felt. The comfort of the carbon felt as a respiratory filtration layer was determined

through breathability and water vapor permeability tests. Filtration efficiency and antibacterial testing results indicated that the carbon felt achieved over 90% filtration efficiency for inhalable particles and effectively inhibited microbial growth due to its antibacterial properties. This method of reusing waste textiles maintains consistency in the use of textiles before and after reuse, simplifying the recycling process of waste acrylic fibers while reducing the manufacturing cost of respiratory filters. The designed respiratory filter has immense potential for applications in various environments, including hospitals and virology research institutes.

Future work

- Using molten salt-assisted carbonization method to increase the porosity and specific surface area of the resulting carbon felt.
- A ramping heating strategy may be employed during the carbonization stage to further improve the mechanical properties of the carbon felt.
- Refining the load during the carbonization process to apply tension as uniformly as possible across the fibers.

7 References

[1] Khayyam H., et al., PAN Precursor Fabrication, Applications and Thermal Stabilization Process in Carbon Fiber Production: Experimental and Mathematical Modelling. *Progress in Materials Science*, 2020, 107, 100575, https://doi.org/10.1016/j.pmatsci.2019.100575.

[2] Kopeć M., et al., Polyacrylonitrile-Derived Nanostructured Carbon Materials. *Progress in Polymer Science*, 2019, 92, 89–134, https://doi.org/10.1016/j.progpolymsci.2019.02.003.

[3] Brown K.R., et al., Carbon Fibers Derived from Commodity Polymers: A Review. *Carbon*, 2022, 196, 422–39, https://doi.org/10.1016/j.carbon.2022.05.005.

[4] Su Y., et al., Application of Modified Graphite Felt as Electrode Material: A Review. *Carbon Letters*, 2023, 33, no. 1, 1–16, https://doi.org/10.1007/s42823-022-00414-x.

[5] Huong Le T.X., et al., Carbon Felt Based-Electrodes for Energy and Environmental Applications: A Review. *Carbon*, 2017, 122, 564–91, https://doi.org/10.1016/j.carbon.2017.06.078.

[6] He Zhangxing, et al., Effects of Nitrogen Doping on the Electrochemical Performance of Graphite Felts for Vanadium Redox Flow Batteries. *International Journal of Energy Research*, 2015, 39, no. 5, 709–16, https://doi.org/10.1002/er.3291.

[7] Chen T., et al., Effects of Needle-Punched Felt Structure on the Mechanical Properties of Carbon/Carbon Composites. *Carbon*, 2003, 41, no. 5, 993–99, https://doi.org/10.1016/S0008-6223(02)00445-1.

[8] Jiang T., et al., Highly Thermally Conductive and Negative Permittivity Epoxy Composites by Constructing the Carbon Fiber/Carbon Networks. *Composites Communications*, 2023, 39, 101560, https://doi.org/10.1016/j.coco.2023.101560.

[9] Singh K., and V. Baheti, Electromagnetic Interference Shielding and Ohmic Heating Applications of Carbonized Nonwoven Fabrics Prepared from Blended Fibrous Wastes. *Diamond and Related Materials*, 2023, 133, 109708, https://doi.org/10.1016/j.diamond.2023.109708.

[10] Xia M., et al., Conversion of Cotton Textile Wastes into Porous Carbons by Chemical Activation with ZnCl2, H3PO4, and FeCl3. *Environmental Science and Pollution Research*, 2020, 27, no. 20, 25186–96, https://doi.org/10.1007/s11356-020-08873-3.

[11] Tian D., et al., Multifaceted Roles of FeCl2 on Pore Formation of Polyester Fabric Wastes-Based Activated Carbon. *Colloids and Surfaces A: Physicochemical and Engineering Aspects*, 2020, 598, no. February, 124756, https://doi.org/10.1016/j.colsurfa.2020.124756.

[12] Nahil M.A., and P.T. Williams, Activated Carbons from Acrylic Textile Waste. *Journal of Analytical and Applied Pyrolysis*, 2010, 89, no. 1, 51–59, https://doi.org/10.1016/j.jaap.2010.05.005.

[13] --- Surface Chemistry and Porosity of Nitrogen-Containing Activated Carbons Produced from Acrylic Textile Waste. *Chemical Engineering Journal*, 2012, 184, 228–37, https://doi.org/10.1016/j.cej.2012.01.047.

[14] Chen W., et al., Pyrolysis Behavior and Pore-Forming Mechanism During Reuse of Textile

Waste Flax by Activation. *Waste and Biomass Valorization*, 2020, 11, no. 8, 4259–68, https://doi.org/10.1007/s12649-019-00770-2.

[15] Gu S., et al., Fabrication of Porous Carbon Derived from Cotton/Polyester Waste Mixed with Oyster Shells: Pore-Forming Process and Application for Tetracycline Removal. *Chemosphere*, 2021, 270, 129483, https://doi.org/10.1016/j.chemosphere.2020.129483.

[16] Salim N. V., et al., The Role of Tension and Temperature for Efficient Carbonization of Polyacrylonitrile Fibers: Toward Low Cost Carbon Fibers. *Industrial and Engineering Chemistry Research*, 2018, 57, no. 12, 4268–76, https://doi.org/10.1021/acs.iecr.7b05336.

[17] Xu J., et al., Effect of Tension during Stabilization on Carbon Fiber Multifunctionality for Structural Battery Composites. *Carbon*, 2023, 209, 117982, https://doi.org/10.1016/j.carbon.2023.03.057.

[18] Liu Y., et al., Gel-Spun Carbon Nanotubes/Polyacrylonitrile Composite Fibers. Part III: Effect of Stabilization Conditions on Carbon Fiber Properties. *Carbon*, 2011, 49, no. 13, 4487–96, https://doi.org/10.1016/j.carbon.2011.06.045.

[19] Rahaman M.S.A., et al., A Review of Heat Treatment on Polyacrylonitrile Fiber. *Polymer Degradation and Stability*, 2007, 92, no. 8, 1421–32, https://doi.org/10.1016/j.polymdegradstab.2007.03.023.

[20] Naeem S., et al., Development of Porous and Electrically Conductive Activated Carbon Web for Effective EMI Shielding Applications. *Carbon*, 2017, 111, 439–47, https://doi.org/10.1016/j.carbon.2016.10.026.

[21] Wu M., et al., Optimization of Stabilization Conditions for Electrospun Polyacrylonitrile Nanofibers. *Polymer Degradation and Stability*, 2012, 97, no. 8, 1511–19, https://doi.org/10.1016/j.polymdegradstab.2012.05.001.

[22] Santos de Oliveira Junior M., et al., A Statistical Approach to Evaluate the Oxidative Process of Electrospun Polyacrylonitrile Ultrathin Fibers. *Journal of Applied Polymer Science*, 2017, 134, no. 43, 45458, https://doi.org/10.1002/app.45458.

[23] Sabantina L., et al., Stabilization of Electrospun PAN/Gelatin Nanofiber Mats for Carbonization. *Journal of Nanomaterials*, 2018, 2018, 1–12, https://doi.org/10.1155/2018/6131085.

[24] Nan W., et al., Mechanically Flexible Electrospun Carbon Nanofiber Mats Derived from Biochar and Polyacrylonitrile. *Materials Letters*, 2017, 205, 206–10, https://doi.org/10.1016/j.matlet.2017.06.092.

[25] Storck J.L., et al., Metallic Supports Accelerate Carbonization and Improve Morphological Stability of Polyacrylonitrile Nanofibers during Heat Treatment. *Materials*, 2021, 14, no. 16, 4686, https://doi.org/10.3390/ma14164686.

[26] --- Comparative Study of Metal Substrates for Improved Carbonization of Electrospun PAN Nanofibers. *Polymers*, 2022, 14, no. 4, 721, https://doi.org/10.3390/polym14040721.

[27] Fridrichová L., A New Method of Measuring the Bending Rigidity of Fabrics and Its Application to the Determination of the Their Anisotropy. *Textile Research Journal*, 2013, 83, no. 9, 883–92, https://doi.org/10.1177/0040517512467133.

[28] Yang T., et al., Study on the Sound Absorption Behavior of Multi-Component Polyester Nonwovens: Experimental and Numerical Methods. *Textile Research Journal*, 2019, 89, no. 16, 3342–61, https://doi.org/10.1177/0040517518811940.

[29] Xiong X., et al., Transport Properties of Electro-Sprayed Polytetrafluoroethylene Fibrous Layer Filled with Aerogels/Phase Change Materials. *Nanomaterials*, 2020, 10, no. 10, 2042, https://doi.org/10.3390/nano10102042.

[30] Acem Z., et al., Surface Temperature of Carbon Composite Samples during Thermal Degradation. *International Journal of Thermal Sciences*, 2017, 112, 427–38, https://doi.org/10.1016/j.ijthermalsci.2016.11.007.

[31] Peng Q., et al., Preparation of Electrosprayed Composite Coated Microporous Filter for Particulate Matter Capture. *Nano Select*, 2022, 3, no. 3, 555–66, https://doi.org/10.1002/nano.202100186.

[32] Hong X., and D.D.L. Chung, Carbon Nanofiber Mats for Electromagnetic Interference Shielding. *Carbon*, 2017, 111, 529–37, https://doi.org/10.1016/j.carbon.2016.10.031.

[33] Pei X., et al., Porous Network Carbon Nanotubes/Chitosan 3D Printed Composites Based on Ball Milling for Electromagnetic Shielding. *Composites Part A: Applied Science and Manufacturing*, 2021, 145, 106363, https://doi.org/10.1016/j.compositesa.2021.106363.

[34] Liang J., et al., Electromagnetic Shielding Property of Carbon Fiber Felt Made of Different Types of Short-Chopped Carbon Fibers. *Composites Part A: Applied Science and Manufacturing*, 2019, 121, no. March, 289–98, https://doi.org/10.1016/j.compositesa.2019.03.037.

[35] Zhang M., et al., Theoretical Prediction of Effective Stiffness of Nonwoven Fibrous Networks with Straight and Curved Nanofibers. *Composites Part A: Applied Science and Manufacturing*, 2021, 143, 106311, https://doi.org/10.1016/j.compositesa.2021.106311.

[36] Chen J., et al., The Catalytic Effect of Boric Acid on Polyacrylonitrile-Based Carbon Fibers and the Thermal Conductivity of Carbon/Carbon Composites Produced from Them. *Carbon*, 2010, 48, no. 8, 2341–46, https://doi.org/10.1016/j.carbon.2010.03.012.

[37] Naito K., et al., Enhancing the Thermal Conductivity of Polyacrylonitrile- and Pitch-Based Carbon Fibers by Grafting Carbon Nanotubes on Them. *Carbon*, 2010, 48, no. 6, 1849–57, https://doi.org/10.1016/j.carbon.2010.01.031.

[38] Zhang Y., et al., Rapid In Situ Polymerization of Polyacrylonitrile/Graphene Oxide Nanocomposites as Precursors for High-Strength Carbon Nanofibers. *ACS Applied Materials & Interfaces*, 2021, 13, no. 14, 16846–58, https://doi.org/10.1021/acsami.1c02643.

[39] Šafářová V., and J. Militký, Electromagnetic Shielding Properties of Woven Fabrics Made from High-Performance Fibers. *Textile Research Journal*, 2014, 84, no. 12, 1255–67, https://doi.org/10.1177/0040517514521118.

[40] Schuepfer D.B., et al., Assessing the Structural Properties of Graphitic and Non-Graphitic Carbons by Raman Spectroscopy. *Carbon*, 2020, 161, 359–72, https://doi.org/10.1016/j.carbon.2019.12.094.

[41] Cheng H., et al., Ultrathin Flexible Poly(Vinylidene Fluoride)/MXene/Silver Nanowire Film with Outstanding Specific EMI Shielding and High Heat Dissipation. *Advanced Composites*

and Hybrid Materials, 2021, 4, no. 3, 505–13, https://doi.org/10.1007/s42114-021-00224-1.

[42] Pande S., et al., Mechanical and Electrical Properties of Multiwall Carbon Nanotube/Polycarbonate Composites for Electrostatic Discharge and Electromagnetic Interference Shielding Applications. *RSC Advances*, 2014, 4, no. 27, 13839, https://doi.org/10.1039/c3ra47387b.

[43] Al-Saleh M.H., et al., EMI Shielding Effectiveness of Carbon Based Nanostructured Polymeric Materials: A Comparative Study. *Carbon*, 2013, 60, 146–56, https://doi.org/10.1016/j.carbon.2013.04.008.

[44] Agnihotri N., et al., Highly Efficient Electromagnetic Interference Shielding Using Graphite Nanoplatelet/Poly(3,4-Ethylenedioxythiophene)–Poly(Styrenesulfonate) Composites with Enhanced Thermal Conductivity. *RSC Advances*, 2015, 5, no. 54, 43765–71, https://doi.org/10.1039/C4RA15674A.

[45] Yan D.-X., et al., Efficient Electromagnetic Interference Shielding of Lightweight Graphene/Polystyrene Composite. *Journal of Materials Chemistry*, 2012, 22, no. 36, 18772, https://doi.org/10.1039/c2jm32692b.

[46] Song W.-L., et al., Flexible Graphene/Polymer Composite Films in Sandwich Structures for Effective Electromagnetic Interference Shielding. *Carbon*, 2014, 66, 67–76, https://doi.org/10.1016/j.carbon.2013.08.043.

[47] Moglie F., et al., Electromagnetic Shielding Performance of Carbon Foams. *Carbon*, 2012, 50, no. 5, 1972–80, https://doi.org/10.1016/j.carbon.2011.12.053.

[48] Ji K., et al., Fabrication and Electromagnetic Interference Shielding Performance of Open-Cell Foam of a Cu–Ni Alloy Integrated with CNTs. *Applied Surface Science*, 2014, 311, 351–56, https://doi.org/10.1016/j.apsusc.2014.05.067.

[49] Ji S., et al., Thermal Response of Transparent Silver Nanowire/PEDOT:PSS Film Heaters. *Small*, 2014, 10, no. 23, 4951–60, https://doi.org/10.1002/smll.201401690.

[50] Chu K., et al., Electrical and Thermal Properties of Carbon-Nanotube Composite for Flexible Electric Heating-Unit Applications. *IEEE Electron Device Letters*, 2013, 34, no. 5, 668–70, https://doi.org/10.1109/LED.2013.2249493.

[51] Sui D., et al., Flexible and Transparent Electrothermal Film Heaters Based on Graphene Materials. *Small*, 2011, 7, no. 22, 3186–92, https://doi.org/10.1002/smll.201101305.

[52] Wang Q., et al., Multifunctional and Water-Resistant MXene-Decorated Polyester Textiles with Outstanding Electromagnetic Interference Shielding and Joule Heating Performances. *Advanced Functional Materials*, 2019, 29, no. 7, https://doi.org/10.1002/adfm.201806819.

[53] Abraham J.P., et al., Using Heat to Kill SARS-CoV-2. *Reviews in Medical Virology*, 2020, 30, no. 5, https://doi.org/10.1002/rmv.2115.

8 List of papers published by the author

8.1 Publications in journals

[1] **Wang, Y**., Hu, S., Tunáková, V., Niamlang, S., Chvojka, J., Venkataraman, M., ... & Ali, A. (2024). Carbon felt from acrylic dust bags as flexible EMI shielding layer and resistive heater. Journal of Materials Research and Technology, 28, 4417-4427.

[2] **Wang, Y**., Baheti, V., Yang, K., Yang, T., Wiener, J., & Militký, J. (2021). Utility of whiskerized carbon fabric surfaces in resistive heating of composites. Polymer Composites, 42(6), 2774-2786.

[3] **Wang, Y**., Baheti, V., Khan, M. Z., Viková, M., Yang, K., Yang, T., & Militký, J. (2022). A facile approach to develop multifunctional cotton fabrics with hydrophobic, self-cleaning and UV protection properties using ZnO particles and fluorocarbon. The Journal of The Textile Institute, 113(10), 2238-2248.

[4] **Wang, Y**., Khan, M. Z., Li, S., Novotná, J., Viková, M., Stuchlík, M., ... & Petru, M. (2023). A novel approach to fabricate durable superhydrophobic and UV protective cotton fabrics using fly ash and graphene nanoplatelets. Cellulose, 1-16.

[5] **Wang, Y**. F., Baheti, V., Yang, K., Venkataraman, M., & Yang, T. (2020). Study on Ohmic Heating Behavior of Fly Ash Filled Carbon Woven/Epoxy Resin Composite. Journal of Fiber Bioengineering and Informatics, 13(1), 1-11.

[6] Yang, T., Hu, L., Xiong, X., **Wang, Y**., Wang, X., Petrů, M., ... & Militký, J. (2021). A comparison of fabric structures for carbon fiber reinforced composite: Laminated and orthogonal woven structures. Polymer Composites, 42(10), 5300-5309.

[7] Peng, Q., Tan, X., Xiong, X., **Wang, Y**., Novotná, J., Shah, K. V., ... & Militky, J. (2023). Insights into the large‐size graphene improvement effect of the mechanical properties on the epoxy/glass fabric composites. Polymer Composites, 44(11), 7430-7443.

[8] Yang, T., Xiong, X., **Wang, Y**., Mishra, R., Petrů, M., & Militký, J. (2021). Application of acoustical method to characterize nonwoven material. Fibers and Polymers, 22, 831-840.

[9] Yang, K., Zhang, X., Venkataraman, M., Chen, K., **Wang, Y**., Wiener, J., ... & Militky, J. (2024). Thermal behavior of flexible and breathable sandwich fibrous polyethylene glycol (PEG) encapsulations. Textile Research Journal, 00405175241236494.

[10] Yang, K., Wiener, J., Venkataraman, M., **Wang, Y**., Yang, T., Zhang, G., ... & Militky, J. (2021). Thermal analysis of PEG/Metal particle-coated viscose fabric. Polymer Testing, 100, 107231.

[11] Karthik, D., Militky, J., **Wang, Y**., & Venkataraman, M. (2023). Joule Heating of Carbon-Based Materials Obtained by Carbonization of Para-Aramid Fabrics. C, 9(1), 23.

[12] Hu, S., Wang, D., Venkataraman, M., Křemenáková, D., Militký, J., Yang, K., **Wang Y**., Palanisamy, S. (2023). Enhanced electromagnetic shielding of lightweight copper-coated nonwoven laminate with carbon filament reinforcement. Journal of Engineered Fibers and Fabrics, 18, 15589250231199970.

[13] Ali, A., Azeem, M., Noman, M. T., Amor, N., Militky, J., Petru, M., & **Wang, Y**. (2022). Development of silver plated electrically conductive elastomers embedded with carbon black particles obtained from Kevlar waste source. Polymer Testing, 116, 107793.

[14] Yang, K., Zhang, X., Wiener, J., Venkataraman, M., **Wang, Y**., Zhu, G., ... & Militky, J. (2022). Nanofibrous membranes in multilayer fabrics to avoid PCM leakages. ChemNanoMat, 8(10), e202200352.

[15] Baheti, V., & **Wang, Y**. (2021). Ohmic heating and mechanical stability of carbon fabric/green epoxy composites after incorporation of fly ash particles. Materials Today Communications, 26, 101710.

[16] Khan, M. Z., Militky, J., Petru, M., Ali, A., **Wang, Y**., & Kremenakova, D. (2021). Hydrothermal Growth of TiO2 Nanoflowers on PET Fabrics for Functional Applications. Journal of Fiber Bioengineering and Informatics, 14(4), 199-210.

[17] Yang, K., Venkataraman, M., Karpiskova, J., Suzuki, Y., Ullah, S., Kim, I. S., ... & Yao, J. (2021). Structural analysis of embedding polyethylene glycol in silica aerogel. Microporous and Mesoporous Materials, 310, 110636.

[18] Yang, K., Venkataraman, M., **Wang, Y. F**., Xiong, X. M., Yang, T., Wiener, J., ... & Yao, J. M. (2020). Thermal performance of a multi-layer composite containing peg/laponite as pcms. Journal of Fiber Bioengineering and Informatics, 13(2), 61-68.

8.2 Contribution in conference proceeding

[1**] Wang Y**.-F., Karthik D., Yang K., Yang T., Xiong X.-M., Baheti V., Militký J. Electrical heating properties of carbon fabric/green epoxy composites filled with fly ash (2019) Textile Bioengineering and Informatics Symposium Proceedings 2019 - 12th Textile Bioengineering and Informatics Symposium, TBIS 2019, pp. 44 – 51.

[2] **Y.-F. Wang**, V. Baheti, K. Yang, S. Hu, D. Wang, X.-D. Tan, T. Yang and J. Militký, "Electrical heating properties of various carbonized textile structures," in: Text. Bioeng. Informatics Symp. Proc. 2020 - 13th Text. Bioeng. Informatics Symp. TBIS 2020, pp. 99–106, 2020.

[3] **Y.-F. Wang**, J. Militky, A.P. Periyasamy, M. Venkataraman, V. Baheti, K. Yang, S. Hu, D. Wang, X.-D. Tan, T. Yang, T. Yang and Q.-Y. Peng, "Disinfection mechanisms of UV light and

ozonization," Text. Bioeng. Informatics Symp. Proc. 2020 - 13th Text. Bioeng. Informatics Symp. TBIS 2020, pp. 173–180, 2020.

[4] **Y. Wang,** M. Venkataraman, V. Baheti, K. Yang, T. Yang, S. Hu, J. Wiener, J. Militký, Structural stability of carbon fiber composite heating elements functionalized with ZnO whiskers. Autex Conference 2021.

[5] **Wang Y.-F**., Venkataraman M., Peng Q.-Y., Yang K., Hu S., Militký J. Development of Polydimethylsiloxane (PDMS) /Copper-coated Graphite Elastomer for Strain Sensors (2022) Textile Bioengineering and Informatics Symposium Proceedings 2022 - 15th Textile Bioengineering and Informatics Symposium, TBIS 2022, pp. 8 – 15.

[6] **Wang, Yuanfeng**, Mohanapriya Venkataraman, and Jiri Militky. "Resistive heating performance of waste cotton-derived carbon obtained by salt-assisted hydrothermal carbonization." AUTEX 2022: 21st World Textile Conference AUTEX 2022-AUTEX Conference Proceedings, Lodz University of Technology Press, Lodz 2022, ISBN 978-83-66741-75-1.

8.3 Quotation

Eventual citation of the leading citation databases (Web of Science, Scopus).

Curriculum Vitae

Yuanfeng Wang | Ph.D. student

Faculty of Textile Engineering

Technical University of Liberec

Email: yuanfeng.wang@tul.cz

Profile

As a Ph.D. candidate specializing in Textile Engineering, my research focuses on development of flexible carbon structures from textile materials. My research experience has equipped me with advanced expertise in materials preparation with a focus on precise parameter control. I have also gained significant experience in the characterization of fiber materials and innovative methods for fiber material modification to enhance multifunctionality. I am committed to applying this knowledge to further advancements in the development of flexible carbon materials.

Research Experience

Participated as group leader in Student Grant Competition (SGS) project.

- Functionalized carbon structures for textile applications (SGS-2019-6057).
- Advanced surface modifications of carbon fibers (SGS-2020-6040).
- Doped carbon structures with enhanced surface area and joule heating (SGS-2021-6008).

Participated as group member in Student Grant Competition (SGS) project.

- Carbon particles doping for preparation of conductive composites with enhanced mechanical properties (SGS-2022-6031).

Internship Experience

Sep. 2019 - Nov. 2019: National Taipei University of Technology

Jun. 2021- Aug. 2021: Večerník s.r.o.

Jan. 2023-Feb. 2023: Rajamangala University of Technology Thanyaburi

Brief description of the current expertise, research and scientific activities

Doctoral studies	
Studies	Textile Engineering Textile Technics and Materials Engineering full time
Exams	Structure and Properties of Tex. Fibers, 03.05.18 Mathematical Statistics and Data Analysis, 27.06.18 Heat and Mass Transfer in Porous Media, 15.01.19 Theoretical Textile Metrology, 14.05.20 Experimental technique of the textile, 14.01.22
SDE	State Doctoral Exam completed on 05.12.2023 with the overall result passed.
Teaching Activities	
Teaching	-
Leading Bachelors/ Master students	-
Research projects	Functionalized carbon structures for textile applications(SGS-2019-6057), project leader, 2019. Advanced surface modifications of carbon fibers (SGS-2020-6040), project leader, 2020.

	Doped carbon structures with enhanced surface area and joule heating (SGS-2021-6008), project leader,2021. Carbon particles doping for preparation of conductive composites with enhanced mechanical properties (SGS-2022-6031), project member, 2022.
Other projects	-

Reccomedation of the supervisor

Recommendation of the supervisor

Thesis title: Multifunctional carbon based felt
Author: Yuanfeng Wang, M.Eng.

The PhD thesis of Yuanfeng Wang is concerned with the utilization of pyrolysis under special conditions for transformation of waste acrylic felt coated from one side by PTFE into carbon felt with enhanced multifunctional properties.

The impact of different loading tension methods and PTFE coatings during the pyrolysis process on the shrinkage, mechanical properties, electrical properties, and thermal properties of the resulting carbon felt was comprehensively investigated. The influence of PTFE concentration on the morphology, mechanical properties, and electrical properties of PTFE-coated acrylic felts pyrolysis results was evaluated. The excellent properties of prepared carbon felt were base for construction of filtration layer of a respiratory filters enabling sufficient filtration efficiency and high-temperature electrical disinfection. The design of the mask body and the corresponding electrode configuration were created.

The thesis follows required format and author was successfully realized all of its proposed objectives. The candidate demonstrated a high level of quality of his research and achieved original results during the preparation and characterization of flexible carbon felts. He employed advanced comprehensive scientific methods to measure of felts properties, evaluate of results and examine of data. The discussions of results are deep, complex and include comparisons of the attained results with those of other published works. The language proficiency exhibited in the thesis satisfies the standards expected at the doctoral level. Main parts of his findings exhibit novelty and were published by him in high-impacted academic journals. His exceptional abilities are evident from his publication record in journals with high-impact factors.

Throughout his PhD study at TUL, he has promoted his findings through the publication of 18 papers in journals with impact factors ad 6 articles in conference proceedings. Throughout his academic pursuits, he demonstrated a high level of diligence and competency. The findings of the dissertation are valuable, innovative, and readily applicable in practice. Thus, it is highly recommended that the thesis will be accepted for the final doctoral defense.

Prof. Eng. Jiří Militký CSc, EURING, FEA 22/05/2004
Supervisor

Rewievs of the opponents

OPPONENT'S REVIEW OF THE DISSERTATION

Topic of dissertation thesis:

MULTIFUNCTIONAL CARBON BASED FELT

Thesis author: Yuanfeng Wang, M.Eng, Faculty of Textile Engineering, Department of material engineering, Technical University of Liberec

Opponent: doc. RNDr. Jiří Vaníček, CSc., Previously University of Economics, Faculty of International Relations, Prague

The aim of this thesis is to carbonize acrylic-based waste felts under controlled conditions to produce carbon felt and enable its multifunctional applications. This study aims to investigate the impact of different loading tension methods and PTFE coatings during the pyrolysis process on the shrinkage rate, mechanical properties, electrical properties, and thermal properties of the resulting carbon felt. The results indicate that applying edge load to the samples during the carbonization stage helps to reduce the shrinkage rate of the final product, allowing the carbon felt to gain flexibility and form a well-structured conductive network. By examining the morphology, mechanical properties, and electrical properties of PTFE-coated samples, we found that higher coating concentrations had a greater impact on the performance of the resulting carbon felt. Although high coating concentrations increased the material's modulus and electrical conductivity, they also led to a loss of flexibility in the carbon felt, which could severely limit its application scope. By characterizing the morphology and structure of carbon felts prepared at different carbonization temperatures under an edge loading mode, it was found that increasing the carbonization temperature promoted higher crystallinity within the fibres and the formation of an ordered graphite structure. The formation of a dense, highly conductive network and high porosity was achieved. Additionally, the carbon felt exhibited excellent heating efficiency and high heating rates in resistive heating tests. The results showed that even under heating conditions, the carbon felt could maintain internal conductive pathway stability through multiple bending cycles. This work also investigated the feasibility of converting acrylic -based filter felts into carbon felts for use in respiratory filtration layers. The excellent electrical conductivity of carbon felt allows it to be used not only as a respiratory filtration layer but also for high-temperature electrical disinfection. The design of the mask body and the corresponding electrode configuration enabled controlled resistive heating performance, ensuring the reliability of high-temperature disinfection of the carbon felt. Flexible carbon felt offers lower manufacturing costs and exhibits good chemical and structural stability. Functional testing results indicate that it demonstrates significant potential for applications in wearable heaters, flexible EMI shielding, respiratory filters, and other related fields. The scope of the work is 89 pages. The dissertation is divided into six chapters: Introduction. Objectives. State of the art. Experimental materials and methods. Results and discussion. Conclusion. In the chapter "State of the art" the state of knowledge of the studied issue is analysed in detail. But even in the discussion, the achieved results are always confronted with findings from

the literature. In the chapter "Experimental materials and methods" the used materials and sample preparation and all used methods of evaluation of samples obtained by pyrolysis of felt samples are described. Unbelievable 14 assessment methods were used, requiring a large amount of experimental work. I consider the experimental part of the thesis to be the best part of the whole dissertation. The number of research outputs is respectable. It presents 18 journal papers, 3 book chapters and 6 conference papers. The only thing I would criticize the work for is a small effort to generalize the achieved results.

As part of the dissertation defense, I ask the author to comment on the above comments and take a position on the following questions:

- ✓ Why did you pay so much attention to investigate the impact of different loading tension methods and PTFE coatings during the pyrolysis process, when evaluated practical applications do not use PTFE coatings?
- ✓ Are there any known practical applications of using carbon flats? For example, for applications in wearable heaters, flexible EMI shielding, respiratory filters, and other related fields.
- ✓ In chapter 6.4. "Future work" you propose using molten salt-assisted carbonization method to increase the porosity and specific surface area of the resulting carbon felt. What do you expect from this work and what knowledge is it based on?

Overall evaluation of the work:

The dissertation deals with a very current topic, it brings new knowledge in the part of the overview of the current situation and sources that address this topic, in the formulation of theoretical starting points for managing the knowledge sharing process, and in the empirical part, which contains a number of outputs.

Conclusion:

The submitted dissertation entitled "MULTIFUNCTIONAL CARBON BASED FELT" fulfils the conditions of a creative scientific work for the award of the Ph.D., and therefore, I recommend the submitted dissertation for defense.

In Tábor on June 30, 2024

Doc. RNDr. Jiří Vaníček, CSc.

Review to dissertation titled "Multifunctional Carbon Based Felt"

This thesis is aimed to convert wasted textiles into valuable product, i.e., recycling of acrylic-based felts for multi-functional flexible carbon felts, which is significant for environmental protection and sustainable development.

Generally, carbon felts have less flexibility, which limits its performance and applications. This thesis work proposed a novel method to improve the flexibility carbon felts by coating polytetrafluoroethylene (PTFE) on it, and this novel method works. Besides, in this thesis work, the functionality of carbon felts in filtration, electrical disinfection, EMI shielding, and electrical heating was achieved. Therefore, this thesis work has its original novelty, as well as a relatively comprehensive investigation on its developed product.

In the introduction section, the literature review covers carbon materials, carbon materials from textile waste, the mechanical properties and applications of carbonized fiber networks at the current state, including the achievements and challenges, which provide a relatively clear picture of relevant research area, and also provide a solid theoretical foundation for the thesis work.

In the experimental section, needle-punched acrylic-based dust filter felt was used as precursor material, and then the precursor material was coated by PTFE, specifically, the precursor material was immersed in PTFE dispersions of different concentrations; subsequently, the PTFE coated precursor materials went through carbonization under specific conditions to be carbon felts. The evaluation of carbon felts in morphology, mechanical properties, porosity, air and water vapor permeability, thermal properties, electrical conductivity, resistive heating, filtration efficiency, EMI shielding effectiveness, structural stability, antibacterial properties were carried out. The methodology was appropriate, the experiments were well-designed, and the description of experimental process and conditions was clear.

In the results and discussion section, the results are presented clearly and the correlations between independent and dependent variables were discussed, for instance, different load modes vs. shrinkage and morphology & mechanical properties & thermal properties & electrical properties, PTFE coating vs. shrinkage and morphology & mechanical properties & electrical conductivity. The results support the conclusions.

Generally speaking, this thesis is written concisely, systematically, logically and well-structured, and provides its novelty and contribution to carbon based felts for multi-purpose application. During the Ph.D. study, the candidate has published 18 papers in journals (5 of them are listed as first author), 3 book chapters, 6 conference papers, which indicates that the candidate has contributed a good

research on his thesis area and got the recognition by peer review. Therefore, I recommend the Ph.D. thesis for defence.

Apart from the above comments, there are some small questions,

1. Except from the PTFE concentration, the mass ratio of PTFE to acrylic-based felt could also be helpful for understanding how the PTFE influence the property of carbon felt. It could also be another correlation between the mass increase of acrylic-based felt and the concentration of dispersion.
2. In section 4.2.2, It mentions that “after thorough saturation, excess dispersion was removed using pressure rollers”, the word “saturation” cannot express precise information, the pressure and the gap between rollers are not clear.
3. The candidate mentioned that the carbon felt is flexible. However, it did not give information about how to define the flexibility.
4. Can the candidate explain the curve AC_800 in Figure 5.36.
5. In Figure 5.39, there is no information for disinfection. Therefore, it could be better to mention that the disinfection could be potential property or application.

Reviewer:

Prof. Lin Liu

School of Materials Science and Engineering

Zhejiang Sci-Tech University